AD_____

Award Number: DAMD17-99-1-9100

TITLE: Mechanism of Action of Substituted Indanones in Multidrug Resistant Breast Cancer

PRINCIPAL INVESTIGATOR: Lorenzo M. Leoni, Ph.D.

CONTRACTING ORGANIZATION: The University of California, San Diego
La Jolla, California 92093-0934

REPORT DATE: September 2001

TYPE OF REPORT: Annual Summary

PREPARED FOR: U.S. Army Medical Research and Materiel Command
Fort Detrick, Maryland 21702-5012

DISTRIBUTION STATEMENT: Approved for Public Release;
Distribution Unlimited

The views, opinions and/or findings contained in this report are those of the author(s) and should not be construed as an official Department of the Army position, policy or decision unless so designated by other documentation.

REPORT DOCUMENTATION PAGE

Form Approved
OMB No. 074-0188

1. AGENCY USE ONLY (Leave blank)	2. REPORT DATE	3. REPORT TYPE AND DATES COVERED
	September 2001	Annual Summary (30 Sep 00 - 31 Aug 01)

4. TITLE AND SUBTITLE
Mechanism of Action of Substituted Indanones in Multidrug Resistant Breast Cancer

5. FUNDING NUMBERS
DAMD17-99-1-9100

6. AUTHOR(S):
Lorenzo M. Leoni, Ph.D.

7. PERFORMING ORGANIZATION NAME(S) AND ADDRESS(ES)
The University of California, San Diego
La Jolla, California 92093-0934

E-Mail: lleoni@ucsd.org

8. PERFORMING ORGANIZATION REPORT NUMBER

9. SPONSORING / MONITORING AGENCY NAME(S) AND ADDRESS(ES)
U.S. Army Medical Research and Materiel Command
Fort Detrick, Maryland 21702-5012

10. SPONSORING / MONITORING AGENCY REPORT NUMBER

11. SUPPLEMENTARY NOTES
Original contains color plates: All DTIC reproductions will be in black and white.

12a. DISTRIBUTION / AVAILABILITY STATEMENT
Approved for Public Release; Distribution Unlimited

12b. DISTRIBUTION CODE

13. ABSTRACT ***(Maximum 200 Words)***

Our laboratory has recently synthesized a series of novel substituted indanones that are selectively toxic to multidrug resistant cancer cells, including breast cancer cell lines.
In this application we proposed to characterize the mechanism of action of indanocine and to assess the in vivo anti-tumor activity of indanocine.
During the second year we:

- published the second report on the biological activity of indanocine (Cancer Res 2001 Oct 1;61(19):7248-54)
- analyzed the indanocine-resistant stable cell line
- identified the potential indanocine-binding site on tubulin
- continued the animal testing of indanocine
- studies the pro-apoptotic mechanism of action in non-dividing tumor cells

The results shown in this annual summary demonstrate that indanocine is a very promising new anti-cancer agent, with selective activity in slowly-dividing or quiescent tumor cells. The positive early animal models suggest that indanocine could be soon ready for clinical trials

14. SUBJECT TERMS:	15. NUMBER OF PAGES
breast cancer	28
	16. PRICE CODE

17. SECURITY CLASSIFICATION OF REPORT	18. SECURITY CLASSIFICATION OF THIS PAGE	19. SECURITY CLASSIFICATION OF ABSTRACT	20. LIMITATION OF ABSTRACT
Unclassified	Unclassified	Unclassified	Unlimited

Table of Contents

Report Year 2001

Introduction

Mechanism of Action of Substituted Indanones in Multidrug Resistant Breast Cancer

Our laboratory has recently synthesized a series of novel substituted indanones that are selectively toxic to multidrug resistant cancer cells, including breast cancer cell lines.
In this application we proposed to characterize the mechanism of action of indanocine and to assess the in vivo anti-tumor activity of indanocine.
During the second year we:

- published the second report on the biological activity of indanocine (Cancer Res 2001 Oct 1;61(19):7248-54)
- analyzed the indanocine-resistant stable cell line
- identified the potential indanocine-binding site on tubulin
- continued the animal testing of indanocine
- studies the pro-apoptotic mechanism of action in non-dividing tumor cells

The results shown in this annual summary demonstrate that indanocine is a very promising new anti-cancer agent, with selective activity in slowly-dividing or quiescent tumor cells. The positive early animal models suggest that indanocine could be soon ready for clinical trials

Body

Task 1

In the first aim of our application, we proposed to characterize further the mechanism of action and the molecular targets of indanocine and related compounds in multidrug resistant breast cancer cell lines. Specifically, we planned to:

9. Develop indanocine resistant breast cancer cell line mutant and assess its pattern of cross resistance to other agents (months 1-24)
10. Characterize biochemically the resistant phenotype, emphasizing cytoskeletal and apoptotic regulatory proteins (months 7-18)
11. Investigate differentially expressed genes in the resistant mutants by human cDNA expression chips (months 12-24)
12. Test the role of the differentially expressed genes by transfection in the wild type cell lines (months 24-32)

Almost all of the specific aims that we planned to investigate in this grant have been addressed by our recently published in Cancer Research (Cancer Res 2001; 61:7248-54). Since the published manuscript is included as an appendix to this annual report, I will refer to it for the experimental details and the major findings.
The most important result in the manuscript is the identification of a tubulin mutation that confers resistance to indanocine in the selected cells. The observed mutation has allowed us to identify a novel tubulin-binding site of indanocine. We plan to use the information generated by these studies to optimize the synthesis of novel indanocine analogs using computer-aided modeling in collaboration with the medicinal chemistry group of Dr. Howard Cottam at UCSD.

The Cancer Research manuscript also reports the surprising finding that indanocine is selectively toxic to non-dividing primary leukemic cells isolated from chronic lymphocytic leukemia (CLL) patients. Since we previously demonstrated that indanocine was able to induce apoptosis in quiescent multidrug resistant breast cancer cell lines (see J Nat Canc Inst, 2000. 92: 217-224), we decided to start studying the killing mechanism in primary tumor cells.

Any anti-cancer agent that is able to selectively induce cell death to non-dividing or slowly dividing tumor cells would represent a great weapon in the cancer chemotherapy arsenal. Indanocine may be used to kill the "quiescent" subset of cancer cells that may not be affected by the conventional chemotherapy.

In the following section we demonstrate the pro-apoptoptic activity of indanocine in primary tumor cells, and we propose a mechanism of action for the killing of non-dividing cells.
When quiescent primary tumor cells are incubated with indanocine, a rapid and potent apoptotic program was activated. Loss of mitochondria transmembrane potential was observed as indicated by the reduction of the DiOC6 staining (Figure 1).

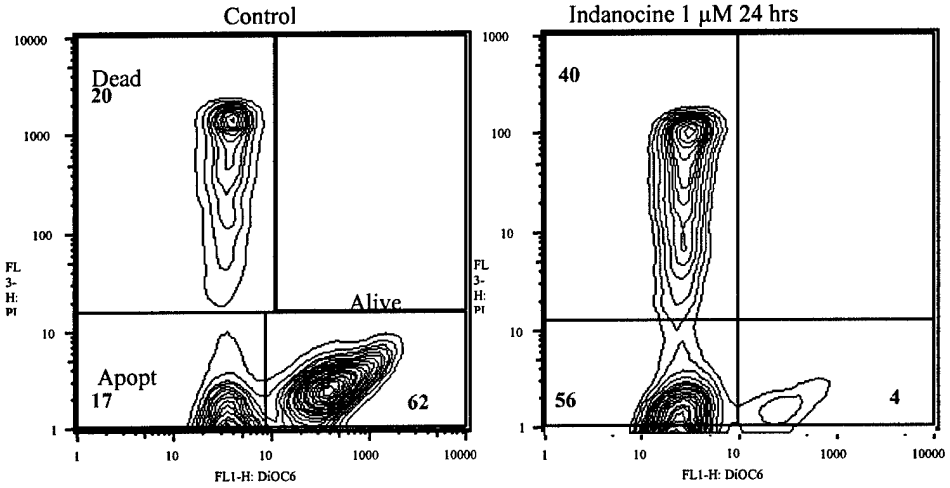

Figure 1. Selective induction of apoptotsis by indanocine in primary tumor cells. Cells were then double stained with DiOC6 and PI, and subject to flowcytometry analysis.

Caspase-3 was rapidly activated after only 2 hour of incubation time point (Figure 2), concomitantly to cytochrome c release from its mitochondrial compartment into the cytosol (dato not shown).

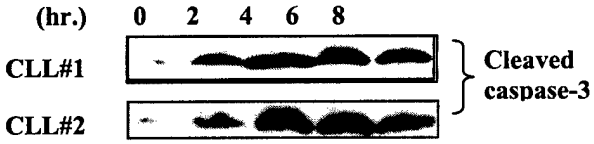

Figure 2. Time course of caspase-3 cleavage. CLL cells were incubated for indicated periods of time with 10μM of indanocine. The cells were then lysed. Cleaved caspase-3 was visualized on Western Blotting using an antibody specific for active caspase-3.

In order to identify the early events activated by indanocine responsible for the activation of the apoptotic program, we investigated the role of the p38 kinase signaling cascade. The p38 kinase has been shown to play an important role in inducing apoptotic cell death. p38 kinase is activated by phosphorylation by the MEK3/6 kinases. The active p38 can phosphorylated and activate transcription factors, such as ATF2. p38 kinase may also activate apoptosis in an transcriptional independent mechanism affecting Bcl-2 family members such as Bax, or facilitating cytochrome c release from mitochondria. In order to test whether p38 kinase was activated by indanocine, we used ATF2 phosphorylation as a surrogate marker of p38 kinase activity. We showed that ATF-2 was phosphorylated at 2 hours following indanocine incubation (Figure 3).

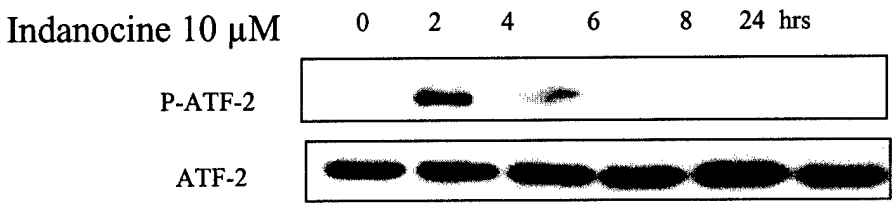

Figure 3. Time course of ATF-2 phosphorylation in tumor cells. Phosphorylation of ATF-2 was visualized by Western Blotting using phosphospecific antibodies (Cell Siganling Inc). Total ATF-2 protein was also shown as control.

The ATF-2 phosphorylation was not observed when normal lymphocytes were incubated with indanocine. Since indanocine do not induce apoptosis in normal lymphocytes, a correlation between killing and ATF-2 phosphorylation was established. This correlation was further corroborated by the finding that paclitaxel, a potent microtubule binding agent, was unable to kill the indanocine-sensitive primary malignant leukemic cells and was also unable to induce ATF-2 phosphorylation (Figure 4).

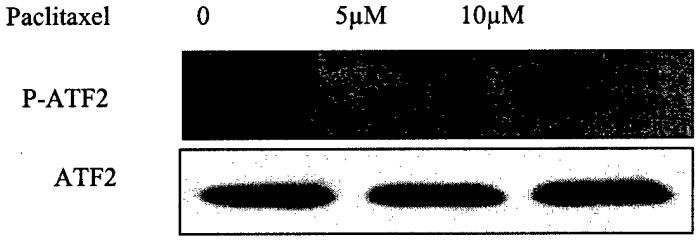

Figure 4. Paclitaxel do not induce ATF-2 phosphorylation in primary leukemic cells. Phosphorylation of ATF-2 was visualized by Western Blotting using phosphospecific antibodies (Cell Siganling Inc). Total ATF-2 protein was also shown as control.

p38 kinase can be phosphorylated and activated by MEK3/6, which is a MAPK kinase (MAPKK). In turn, MEK3/6 can be phosphorylated by mixed lineage kinases (MLK), including the apoptotic signal-regulating kinase 1 (ASK1). Over expression of ASK1 causes apoptotic cell death, and kinase-inactive form of ASK1 blocks the apoptosis induced by tumor necrosis factor-alpha. We discovered that indanocine can activate the ASK1-MEK3/6-p38 kinase cascade (Figure 5.)

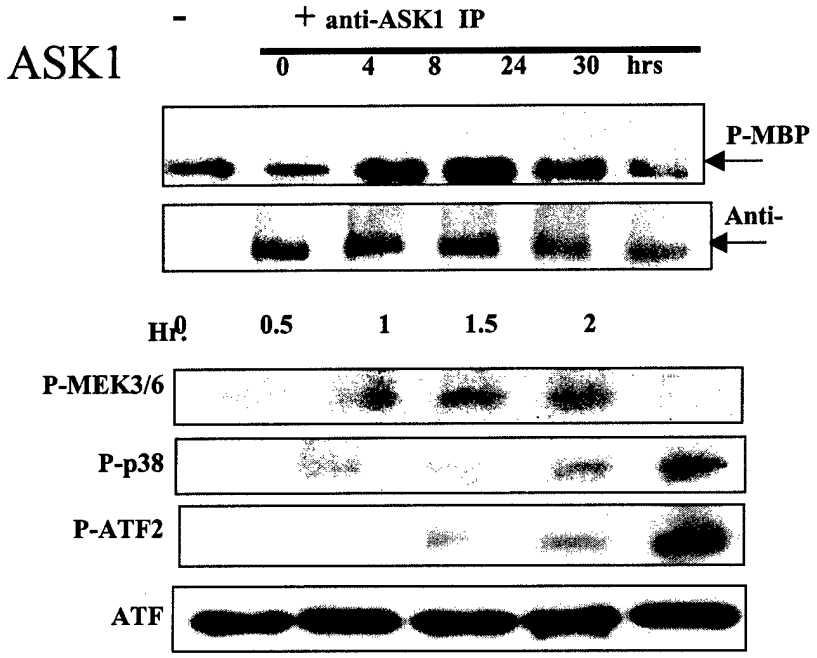

Figure 5. Indanocine activates the ASK1-MEK3/6-p38 kinase-ATF2 signaling cascade. The measure ASK1 activity, cell lysates were subject to immunoprecipitation followed by in vitro kinase assay using MBP as substrates. MBP was strongly phosphorylated at 4 hour. Anti-ASK1 Western blot was also performed to show equal amounts of ASK1 was precipitated. For the detection of MEK3/6, p38 kinase and ATF2, phospho-specific antibodies were used (Cell Signaling Inc).

In living cells, ASK1 is inhibited by thioredoxin. The oxidation of thioredoxin by reactive oxygen species can causes its dissociation from ASK1 and may result in the induction of ASK1 kinase activity. To test this hypothesis we analyzed the levels of reactive oxygen species (ROS) in primary tumor cells after incubation of indanocine. The results we obtained indicate that indanocine can rapidly increase the ROS in the tumor cells (Figure 6).

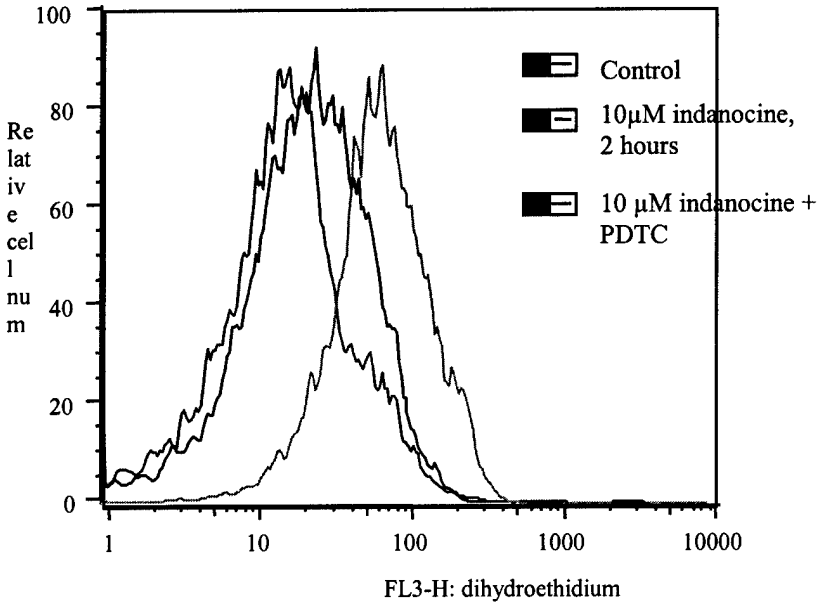

Figure 6. Indanocine increased intracellular O2- production in primary tumor cells.
Tumor cells were incubated with medium alone, 10μM of indanocine, or 10μM indanocine with PDTC for 2 hours. The generation of O2- was quantified by staining the cells with dihydroethidium and analysed by flow cytometry.

In addition, the prevention of ROS formation using the free radical scavenger, Pyrrolidine dithiocarbamate (PDTC), was able to prevent the indanocine-induced ATF2 phosphorylation (Figure 7).

Figure 7. Inhibition of O2- production prevents ATF2 phosphorylation.

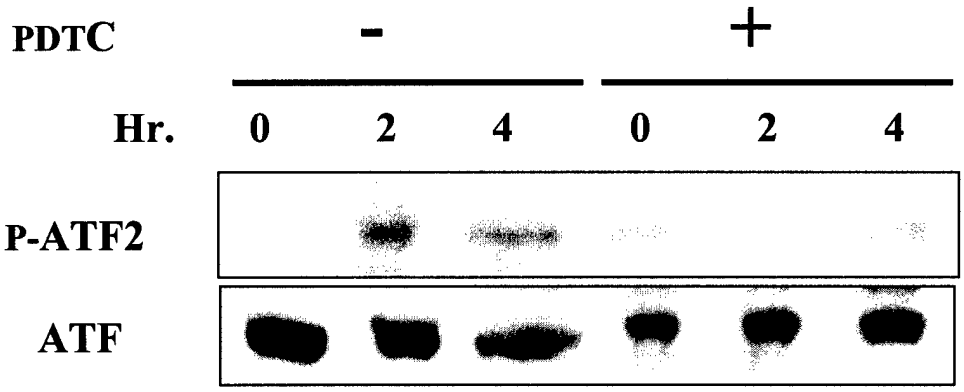

Task 2

In the second aim of the application we proposed to assess the in vivo antitumor activity of indanocine in nude mice bearing multidrug resistant human breast cancer cell lines. Specifically, we planned to:

7. Determine the acute and chronic toxicity of indanocine and related compounds in nude mice.
8. Establish human tumor models in nude mice using wild type, multidrug resistant, and indanocine resistant breast cancer cell lines.
9. Test indanocine and related compounds in the established in vivo tumor models.

The main problem we encountered when testing indanocine in animals was the poor water solubility of the compound. Indanocine can only be prepared in DMSO solutions at a concentration of up to 20 mM concentrations. The highest concentration achievable in acqueous solutions is 100 μM. In order to overcome this problem we generated an indanocine analog that can be solubilized in water and other acqueous solutions (Fig. 8).

Indanorine phosphate can be solubilized in water solutions at concentrations up to 100 mg/ml. The *in*

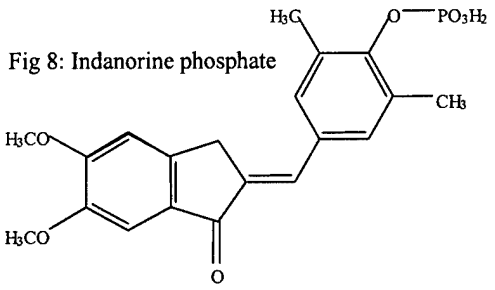

Fig 8: Indanorine phosphate

vitro activity of indanorine phosphate to cancer cell lines was similar, although reduced, to the parenteral compound, indanocine. The bulky and negatively charged phosphate group of indanorine phosphate do not allow the duect penetration through the cell membrane barrier. The difference between the two compounds may be due to the dephosphorylation kinetics.

Cell line	Indanorine phosphate	Indanocine
	IC_{50}, nM	IC_{50}, nM
Jurkat	15	5
MOLT-4	17	7
MCF7	45	20
MCF7/ADR	16	4
MDA-MB-321	35	10
HCT-116	100	55
VM46	100	50
AZ2780	45	30
AZ2780/CD10	30	15

Table 1. Growth-inhibitory activity of indanocine and indanorine phosphate in tumor cell lines. The cells were treated with various concentrations of the indicated drugs for 72 hours. Cell proliferation was assessed with the MTT assay. The results represent the 50% growth-inhibitory concentrations (IC_{50})

Indanorine phosphate also retained its activity against primary quiescent malignant lymphocytes (data not shown).

We used indanorine phosphate for our in vivo assays.

Maximum Tolerated Dose in Athymic Nude Mice

The toxicity of indanorine phosphate was determined in two stages.
(1) The dosage range for the MTD study was determined in a one-mouse dose-escalating study. The drug was administered i.v. in a single dose to a single animal. The dose was then doubled successively for each of the following animals. (2) The MTD study employed two routes of administration, two dosing schedules, and three dosing levels and required twelve groups of mice.
The MTD study indicated that Indanorine phosphate was well tolerated by the athymic nude mice. No MTD was achieved (following NCI guidelines) at concentrations of 100, 200, and 300 mg/kg given i.v. or i.p. at five daily doses (QD x 5) or at five doses given on alternate days (QOD x 5).

In Vivo Evaluation of Indanorine Phosphate against the P388 Murine Leukemia Lines

To evaluate the in vivo efficacy of indanorine phosphate, we tested indanorine phosphate in the P388 murine leukemia model. Female B6D2F1 mice were inoculated on Day 0 with 1 x 106 P388 leukemia cells harvested from tissue culture. As a positive control we used i.p. paclitaxel at 25 mg/kg on a qod x 5 schedule. Indanorine phosphate was dosed at 300 and 500 mg/kg 5 doses QOD. Toxicity was observed at 500 mg/kg and the dose was lowered at 400 mg/kg for the last 3 doses.

Group	n	Primary				Secondary			
		Agent	mg/kg	Route	Schedule	Agent	mg/kg	Route	Schedule
1	10	No Treatment	n/a						
2	10	Paclitaxel	20	IP	QOD x 5				
3	10	SDX-103	500	IP	D 1, 3, 5	SDX-103	400	IP	D 7, 9
4	10	SDX-103	300	IP	QOD x 5				

Table 2. Protocol design of P388 animal model.

Table 3. Summary of the results of P388 animal model.

Group	n	Primary		Secondary		Mean Day of Survival	%T/C	# 30 Day Survival	Max BW. Loss %; (Day)	# of Toxic Deaths
		Agent	mg/kg	Agent	mg/kg	Mean ± SEM (n)				
1	10	No Treatment	n/a			20.7 ± 1.3 (10)	100%	0	---	0
2	10	Paclitaxel	20			27.1 ± 0.8 (8)	131%	0	---	0
3	10	SDX-103	500	SDX-103	400	24.2 ± 1.3 (5)	117%	0	-5.4%; Day 4	2
4	10	SDX-103	300			26 ± 0.8 (9)	126%	0	-2.9%; Day 2	0

Since the NCI cut-off for anti-leukemia activity of an agent in the P388 model is a 120% T/C value or a 20% increase in life span (%ILS), Indanorine phosphate has to be considered active at a dose of 300 mg/kg (T/C 126%). Unfortunately, The T/C ratio is not as high as we may have expected based on the in vitro results.

More assays are currently underway to assess the activity of Indanorine phosphate. In particular we are testing the possibility that indanorine phosphate may have a very short half-life, and therefore, may have to be delivered more frequently. In the current assays we are dosing the drug daily (QD) and twice daily (BID) at 300 mg/kg.

If the results of the current animal assays will be positive we plan to initiate pharmacokinetic and pharmacodynamic studies. Tumor Xenografts in Athymic Nude Mice using human breast cancer cells will then follow, as indicated in the original proposal.

We do not plan to futher pursue assays to determine the in vivo anti-angiogenic or anti-vascular activity of indanocine, before obtaining positive results in the "conventional" tumor models.

Negative results on the new P388 assays (i.e. no increaese in the T/C ratio), will prompt us to test new indanocine analogs that have been prepared for us by the group of Dr. Cottam at UCSD.

Reportable Outcome

Manuscripts

Cancer Res 2001 Oct 1;61(19):7248-54. Biochemical genetic analysis of indanocine resistance in human leukemia.Hua XH, Genini D, Gussio R, Tawatao R, Shih H, Kipps TJ, Carson DA, Leoni LM.

Patent

09/148,576 Carson, Leoni, Cottam and Shih: Novel Anticancer Agents. Claims indanocine and related agents. US Patent Application, European Patent Application # 98958023.8-2112

[CANCER RESEARCH 61, 7248–7254, October 1, 2001]

Biochemical Genetic Analysis of Indanocine Resistance in Human Leukemia[1]

Xuequn Helen Hua, Davide Genini, Rick Gussio, Rommel Tawatao, Hsien Shih, Thomas J. Kipps, Dennis A. Carson, and Lorenzo M. Leoni[2]

Department of Medicine and The Sam and Rose Stein Institute for Research on Aging, University of California, San Diego, La Jolla, California 92093-0663 [X. H. H., D. G., R. T., H. S., T. J. K., D. A. C., L. M. L.], and Target Structure-Based Drug Discovery Group, Information Technology Branch, National Cancer Institute, NIH, Frederick, Maryland 21702 [R. G.]

ABSTRACT

Indanocine is a potent tubulin-binding drug that is cytotoxic to multidrug-resistant cancer cell lines. We demonstrated that indanocine specifically induces apoptosis in malignant B cells from patients with chronic lymphocytic leukemia. To address the exact biochemical basis for indanocine toxicity, an indanocine-resistant clone was selected from mutagenized CEM human lymphoblastoid cells. The resistant cells displayed a stable indanocine-resistant phenotype for at least 9 months in drug-free culture. The cloned cells are cross-resistant to colchicine and vinblastine, but not to paclitaxel, and do not have increased expression of the multidrug-resistant p170 glycoprotein. In both parental cells and cell extracts, indanocine treatment caused tubulin depolymerization. In contrast, the tubulin in the resistant clone did not depolymerize under identical conditions. Both extract mixing and cell fusion experiments suggested that a stable structural change in microtubules, rather than a soluble factor, was responsible for indanocine resistance. Sequence analysis of parental and resistant cells revealed a single point mutation in the M40 isotype of β-tubulin at nucleotide 1050 (G→T, Lys^{350}→Asn) in the indanocine-resistant clone, in a region close to the putative colchicine binding site.

INTRODUCTION

Indanocine is a potent microtubule-depolymerizing agent with antiproliferative activity (1, 2). Indanocine induces apoptotic cell death in a broad range of human tumor cell lines, including several types of multidrug-resistant cells (2). Microtubules are vitally important for cellular functions such as motility, mitosis, and secretion. In cell-free assays using purified tubulin, we showed that indanocine competes with colchicine binding (2), suggesting that the binding sites for indanocine and colchicine are related to each other.

Indanocine is different from many other microtubule-disrupting drugs, because it displays toxicity toward multidrug-resistant cells and kills nondividing or quiescent cells (2). These results suggest that indanocine might work through a mechanism independent of mitotic arrest. Treatment of human malignancies with antitumor agents often results in acquired resistance, which represents a major limitation to chemotherapy. Resistance to the tubulin-binding antimitotic drugs has been shown to be mediated by increased expression of a drug efflux pump, such as Pgp170 (3), by detoxification of the drug in the cell, and by reduced drug influx (4). In addition to these mechanisms, mutational alterations in β-tubulin have been found in paclitaxel- and epothilone-resistant cell lines (5, 6).

To understand the mechanism of indanocine toxicity, an indanocine-resistant clone was derived from the highly sensitive human T-lymphoblastoid CEM cell line. The resistant line displayed weak cross-resistance to colchicine and vinblastine but remained sensitive to paclitaxel. Compared with parental cells, the resistant cells exhibited defective indanocine-driven tubulin depolymerization, both in intact cells and cell-free extracts. The resistant cells had a single point mutation in β-tubulin cDNA that caused a Lys to Asn change at position 350, near the putative colchicine-binding site. These results suggest that altered tubulin structure is one primary cause of indanocine resistance.

MATERIALS AND METHODS

Materials. Indanocine structure is shown in Fig. 2*D*. The compound was synthesized as described (7). Paclitaxel, vinblastine sulfate, colchicine, fludarabine, doxorubicin, staurosporine, and cytochalasin B were purchased from Calbiochem (San Diego, CA) and Sigma Chemical Co. (St. Louis, MO). Unless otherwise designated, all antibodies were purchased from Santa Cruz Biotechnology, Inc. (Santa Cruz Biotechnology, Santa Cruz, CA).

Primary Lymphocyte Assays. This study was approved by the Institutional Review Board of the University of California, San Diego, and all patients gave informed written consent to participation. Patients had to have B-CLL[3] according to National Cancer Institute criteria of any Rai stage. Peripheral blood from CLL patients or normal donors was layered on top of Ficoll-Paque Plus (Pharmacia, Peapack, NJ) and centrifuged at 1200 × *g* for 20 min with break off. The enriched PBMCs were washed three times with Ca^{2+}, Mg^{2+}-free HBSS. Normal B cells were purified from buffy coats using the RosetteSep human B cell kit (StemCell Technologies, Inc., Vancouver, British Columbia, Canada) per the manufacturer's instructions. All primary cells were cultured in RPMI 1640 with 20% fetal bovine serum at a density of 2–5 × 10^6 cell/ml. Freshly isolated CLL cells or normal lymphocytes with viability exceeding 95% or frozen CLL cells with viability exceeding 75% at the time of incubation were used. Because CLL cells display a variable degree of spontaneous apoptosis and for the measurement of the IC_{50} of indanocine at 24 h of incubation, the control cells (treated with vehicle only) were normalized at 100%. With freshly isolated lymphocytes, the viability of the controls at 24 h always exceeded 85%, whereas with the frozen CLL samples the mean viability was 65% (range, 45–85%).

Measurement of Lymphocyte Viability. Lymphocyte viability was assessed by enumeration of cells that excluded erythrosin B. In addition, the percentage of viable cells was assessed by flow cytometry. Briefly, cells were incubated for 10 min at 37°C in culture medium containing 40 nM $DiOC_6$ (Molecular Probes, Eugene, OR) and 5 μg/ml propidium iodide (Molecular Probes), followed by analysis in a Becton Dickinson FACScalibur cytofluorometer. After suitable compensation, fluorescence was recorded at different wavelengths, $DiOC_6$ at 525 nm (FL-1) and PI at 600 nm (FL-3). Viable cells were $DiOC_6$-bright and PI-low.

Cell Culture. The human T-lymphoblastoid CEM cell line came from American Type Culture Collection (CRL-119; Rockwell, MD) and was propagated according to the supplier's instructions in RPMI 1640 supplemented with 10% fetal bovine serum. To select for indanocine-resistant clones, 5 × 10^6 CEM cells were cultured for 18 h in the same medium containing 1 mg/ml of the mutagen ethyl methanesulfonate (Sigma Chemical Co.). Ethyl methanesulfonate was then washed out, and the cells were cultured for 2 days in regular medium. After that the cells were put into medium containing 10 nM indanocine. The concentration of indanocine was raised gradually to keep

Received 4/25/01; accepted 7/26/01.

The costs of publication of this article were defrayed in part by the payment of page charges. This article must therefore be hereby marked *advertisement* in accordance with 18 U.S.C. Section 1734 solely to indicate this fact.

[1] This study is supported by NIH Grants CA 81534 and GM 23200 (to D. A. C.), by Grant DAMD17-99-1-9100 (to L. M. L.) from the Department of Defense, and by a postdoctoral fellowship from the Sass Foundation for Medical Research, Inc. (to X. H. H.).

[2] To whom requests for reprints should be addressed, at Department of Medicine, University of California, San Diego, 9500 Gilman Drive, La Jolla, CA 92093-0663. Phone: (858) 534-5442; Fax: (858) 534-5399; E-mail: lleoni@ucsd.edu.

[3] The abbreviations used are: CLL, chronic lymphocytic leukemia; PBMC, peripheral blood mononuclear cell; $DiOC_6$, 3,3′-dihexyloxacarbocyanine iodide; PI, propidium iodide; MTT, 3-(4,5-dimethylthiazol-2-yl)-2,5-diphenyltetrazolium bromide; Pgp170, P-glycoprotein 170.

Table 1 *Differential sensitivity of normal and malignant B cells to indanocine*

Freshly isolated CLL and normal cells (viability ≥95%) or frozen CLL cells (viability ≥75%) were incubated with increasing concentrations of indanocine ranging from 0.1 to 10 μM for 24 h. The numbers and viabilities of the treated cells were assessed by microscopy and by flow cytometric analysis as described in "Materials and Methods." The IC_{50} is the drug concentration that kills ~50% of the cells. Because CLL cells display a variable degree of spontaneous apoptosis and for the measurement of the IC_{50} of indanocine at 24 h of incubation, the control cells (treated with vehicle only) were normalized at 100%.

Cell type	No. of samples	IC_{50} (μM)
CLL	16	<1
CLL	10	Between 1 and 10
Normal PBMCs	5	>10
Normal B	3	>10

Table 2 *Resistance profile of parental CEM and indanocine-resistant CEM-178 cells*

CEM and CEM-178 cells were continuously exposed to various drugs at serial-diluted concentrations for 72 h. Viable cells were quantified using the MTT assay. The IC_{50} is the drug concentration that inhibited cell growth by 50%.

Drugs	CEM IC_{50}	CEM-178 IC_{50}	CEM:CEM-178
Indanocine	1.79 nM	206 nM	115
Paclitaxel	0.5 nM	0.5 nM	1
Colchicine	2.0 nM	62.5 nM	31
Vinblastine	0.1 nM	4.0 nM	40
Fludarabine	5.8 μM	13.3 μM	2.3
Doxorubicin	0.2 μM	0.4 nM	1.9
Cytochalasin B	7.1 μM	4.6 μM	0.6

viable cells at ~10% of control. The selection was stopped when the resistant variant was able to grow in 300 nM indanocine. The cells were cloned by limiting dilution to yield CEM-178.

Assessment of Cell Growth. The cells were incubated with various concentrations of drugs for 72 h in 96-well plates. Viable cells were quantified by MTT assay, as described (2). The IC_{50} was defined as the concentration of drug required to inhibit cell growth by 50%.

Cellular Assay for Caspase Activity. At the indicated time points, the cells were washed twice with PBS, and the pellets were resuspended in ice-cold caspase buffer [50 mM HEPES (pH 7.4), 100 mM NaCl, 1 mM EDTA, 0.1% 3-[(3-cholamidopropyl)dimethylammonio]-1-propanesulfonate, and 5 mM DTT] and incubated for 10 min on ice. The samples were then centrifuged at 4°C. Supernatant containing 10–20 μg of total protein was aliquoted into 96-well plates. Fifty μl of hypotonic extraction buffer (HEB, contains 50 mM PIPES, 50 mM KCl, 5 mM EGTA, 2 mM $MgCl_2$, 1 mM DTT, and 1 mM phenylmethylsulfonyl fluoride) was mixed with lysates. The reactions were initiated by addition of 100 μM of the specific substrate (Ac-DEVD-AMC for caspase-3 and Ac-LEHD-AFC for caspase-9) acquired from Calbiochem. After 1-h incubation at 37°C, caspase activities were measured by monitoring the released fluorescence of AFC or AMC at excitation and emission wavelengths of 400 and 505 nm, and 380 and 460 nm, respectively.

Measurement of Apoptosis by Cytochrome *c* Release. An early event in apoptosis induced by internal factors is the release into the cytosol of mitochondrial cytochrome *c* (8). Cytosolic and mitochondria cytochrome *c* were separated by extracting cells in HEB buffer (see above) freshly supplemented with 0.1% digitonin (Sigma Chemical Co.). The lysates were vortexed briefly and incubated on ice for 10 min, followed by centrifugation at 16,000 × *g* at 4°C for 5 min. The supernatants and pellets represented cytosolic and mitochondria-associated fractions, respectively. The fractions were then analyzed by Western blotting using anti-cytochrome *c* antibody (PharMingen, San Diego, CA).

Tubulin Polymerization Assay. To quantify tubulin polymerization and depolymerization, an assay was developed by modifying the method of Giannakakou *et al.* (5). For each data point, 2×10^6 of cells were incubated in 2 ml of regular medium containing drugs for various periods of time. The cells were then washed twice at room temperature and resuspended in 50 μl of tubulin extraction buffer (1 mM $MgCl_2$, 2 mM EGTA, 0.5% NP40, and 20 mM Tris-HCl, pH 6.8) supplemented with 2 mM phenylmethylsulfonyl fluoride, and a protease inhibitor cocktail (Sigma Chemical Co.). After a brief but vigorous vortex, the lysates were incubated at room temperature for 5 min and then centrifuged at 16,000 × *g* for 5 min to separate the soluble from polymerized tubulin. The supernatant and pellet fractions were resolved on 10–20% pre-cast Tris-glycine gels (Novex, San Diego, CA) and then subjected to Western blotting with a specific anti-α-tubulin antibody.

Mixing Experiments. Parental CEM cells and the indanocine-resistant clone (CEM-178) were first incubated with 5 μM paclitaxel for 1 h. The cells were then pelleted, washed twice with PBS, and lysed in tubulin extraction buffer. The lysates from CEM and CEM-178 cells were mixed at various proportions. Indanocine (200 μM) was added to the mixed lysate, and the reactions were incubated for 2 h at 37°C. The samples were then spun at 16,000 × *g* for 5 min. Supernatant and pellet fractions were collected and tested by Western blotting.

Cell Fusion Experiment. A hypoxanthine phosphoribosyltransferase-negative and ouabain-resistant CEM cell line was selected as described previously (9). For the fusion experiments, 40×10^6 each of the ouabain-resistant CEM and indanocine-resistant CEM-178 lymphoblasts were mixed in a ratio of 1:1 in serum-free RPMI 1640. Cells were pelleted and incubated for 2 min at 37°C, in 1 ml 50% polyethylene glycol 1500 (PEG 1500; Boehringer Mannheim, Germany) as a fusing agent. Then 1 ml of serum-free RPMI 1640 was dropwise added to the cells at 37°C over 1 min, followed by 7 ml of serum-free RPMI 1640 centrifugation and resuspension at a concentration of 2.5×10^6 cells/ml in regular growth medium. Subsequently, 50 μl of cells were plated in a 96-well plate; the next day, 50 μl of HAT medium (Sigma Chemical Co.) containing 1 μM ouabain (Calbiochem) were added to the cells for double selection. When the cells started to grow, hybridomas resulting from the fusions were selected by limiting dilutions.

Sequence Analysis of Expressed β-Tubulin in CEM-178. Total RNA was extracted from both CEM and CEM-178 using Trizol reagents (Life Technologies, Inc., Gaithersburg, MD) and digested with RNase-free DNase I to eliminate any possible DNA contaminant. cDNA was synthesized by reverse transcription using the Superscript II protocol, followed by RNase H digestion (Life Technologies, Inc.). The cDNA was used as template in PCR reactions with primers specific for the b2 (B1F and B2R) and M40 (M1F and M2R) isotypes of β-tubulin (GenBank accession numbers X02344 and J00314, respectively). The sequences of the primers are shown in Table 3. The PCR was carried out under the following conditions: initial denaturation of 94°C for 12 min, 35 cycles of 94°C 30 s, 48°C (55°C for b2 primers) 30 s, 72°C 80 s, with a final extension at 72°C for 10 min. The resulting 1.2-kb products spanned the full length of the b2 and M40 coding region, except for 17 bp from the 5′ and 3′ ends. The PCR products were purified using Qiagen kits and sequenced by a core facility (The Scripps Research Institute, La Jolla, CA) using the overlapping primers as illustrated in Fig. 5. To avoid PCR errors introduced by Taq polymerase, each PCR reaction was repeated at least once. All of the sequences were verified in both directions.

RESULTS

Differential Sensitivity of Normal and Malignant B Cells to Indanocine. Because it has been reported previously that CLL cells but not normal lymphocytes are highly susceptible to microtubule-binding agents (10), we tested the short-term (24-h) toxicity of in-

Table 3 *Primers used in sequencing b2 and M40 β-tubulin isotypes*

Primer	Sequence
B1F	TTG CAG GCC GGG CAG TG
B2F	AGT GGT GCT GGG AAC AAC T
B3F	CTC GTA GAA AAC ACA GAC GA
B4F	CAA ATG CTT AAT GTC CAA AAC AAA
B5F	CAT GAA CAC GTT TAG TGT GG
B1R	TCG TCT GTG TTT TCT ACG AG
B2R	GGT ACT CGG ACA CCA GGT CA
B3R	CTG ACC GAA AAC GAA GTT GT
B4R	GAG TGG GTC AGC TGG AAA C
M1F	ATC CAG GCT GGT CAA TG
M2F	TCT GGG GCA GGT AAC AAC T
M3F	TTG GTA GAG AAT ACT GAT GA
M4F	CAG ATG CTT AAC GTG CAG AAC AAG
M1R	TCA TCA GTA TTC TCT ACC AA
M2R	GAT ACT CAG AGA CGA GGT CG
M3R	ACC TGT GGC TTC ATT GTA GT

danocine using freshly isolated and frozen cells from 26 CLL patients and from 8 healthy volunteers. All CLL cells were sensitive to indanocine, with IC_{50}s <10 μM. No differences in indanocine sensitivity were encountered between freshly isolated or frozen CLL cells, nor was there a correlation between the indanocine cytotoxicity and the rate of spontaneous apoptosis. In contrast, normal PBMCs or purified normal B cells were resistant to indanocine at concentrations as high as 10 μM (Table 1). The selective cytotoxicity of indanocine observed in CLL cells was attributable to apoptosis, as indicated by subdiploid DNA content, caspase-3 activation, and cytochrome *c* release (data not shown). The results obtained with CLL cells pressed us to study further the mechanism of action of indanocine, by developing indanocine-resistant cells.

Characterization of Indanocine-resistant Lymphoblasts. Compared with parental CEM cells, the CEM-178 clone was 100-fold more resistant to growth inhibition induced by indanocine, with IC_{50}s of 1.79 and 206 nM, respectively (Table 2). The resistant phenotype persisted when the mutant cells were cultured in drug-free medium for at least 9 months. CEM-178 cells grew slightly slower than parental CEM cells, with doubling times of 24 and 18 h, respectively. Quantitative analyses of DNA content by flow cytometry, as well as karyotyping, showed no difference between CEM and CEM-178 (data not shown).

Compared with indanocine, the CEM-178 cells displayed reduced cross-resistance to two other inhibitors of tubulin polymerization, vinblastine (40-fold) and colchicine (31-fold; Table 2). In contrast, CEM-178 was not resistant to the tubulin-polymerizing drug paclitaxel, nor to the cytotoxic agents fludarabine, doxorubicin, and cytochalasin B. These results showed that CEM-178 is specifically resistant to microtubule-depolymerizing agents. Because paclitaxel is a substrate of gp170, the results also suggest that increased drug efflux may not contribute to the resistance. In fact, other experiments showed that the expression of the MDP gp170 was below detection levels in both parental CEM cells and the indanocine-resistant mutant (data not shown).

Most of the CEM cells were killed by $\leq$10 nM indanocine (48 h incubation), whereas CEM-178 cells remained viable after exposure to much higher concentrations (Fig. 1*A*). Indanocine kills an array of cell lines by inducing mitochondria dysfunction, cytochrome *c* release, caspase activation, and apoptosis (2). The drug failed to exert these effects in CEM-178 cells (Fig. 1, *C* and *D*), although the mutant retained functional apoptotic machinery as indicated by activation of caspases when treated with staurosporine (Fig. 1*B*). These results suggest that signaling event(s) upstream of cytochrome *c* release and caspase activation are altered in CEM-178 cells.

Effect of Indanocine on Tubulin Depolymerization. Immunoblotting data indicated that the expression levels of α-tubulin protein were similar between CEM and CEM-178 cells (Fig. 2*A*). To test the possibility that altered tubulin structure might confer indanocine resistance, we evaluated the effect of the drug on the relative levels of polymerized and soluble tubulin in parental and resistant cells. In untreated cells, >99% of the tubulin was in a free, soluble form (Fig. 2*A*). In unmanipulated cells, therefore, it was not possible to quantify an increased amount of soluble form induced by indanocine treatment. However, treatment with 5 μM paclitaxel for 1 h converted all of the tubulin in both CEM and CEM-178 cells into a polymerized form (Fig. 2*A*, + *paclitaxel*). On the basis of these observations, we pretreated the two cell lines with paclitaxel, washed out the drug, and then assayed the effect of indanocine exposure. CEM and CEM-178 cells were preincubated with 5 μM paclitaxel for 1 h, washed twice with drug-free medium, and then incubated with or without 10 μM of indanocine for 2 more h. After harvesting, soluble and polymerized tubulin were separated by centrifugation and assayed by immunoblotting. In wild-type CEM, ~50% of the polymerized tubulin underwent depolymerization after removal of paclitaxel (Fig. 2*B*, *sample #1*). In CEM-178 cells, the majority of tubulin remained in the pellet fraction, and no spontaneous depolymerization occurred (Fig. 2*B*, *sample #3*). When the paclitaxel-treated parental CEM cells were incubated with indanocine, almost all of the tubulin was converted to soluble forms (Fig. 2*B*, *sample #2*). In contrast, paclitaxel-pretreated CEM-178 cells were resistant to the depolymerization effects of indanocine, with >95% of tubulin remaining in the polymerized form (Fig. 2*B*, *sample #4*). To confirm visually the immunoblotting results, the treated cells were also stained with a specific anti-tubulin antibody. Parental CEM and CEM-178 displayed a similar network structure of microtubules after treatment with paclitaxel (Fig. 2*C*, *panels 1* and *3*). Indanocine induced a morphological change only in the parental CEM line, which displayed a diffuse pattern of microtubules, consistent with depoly-

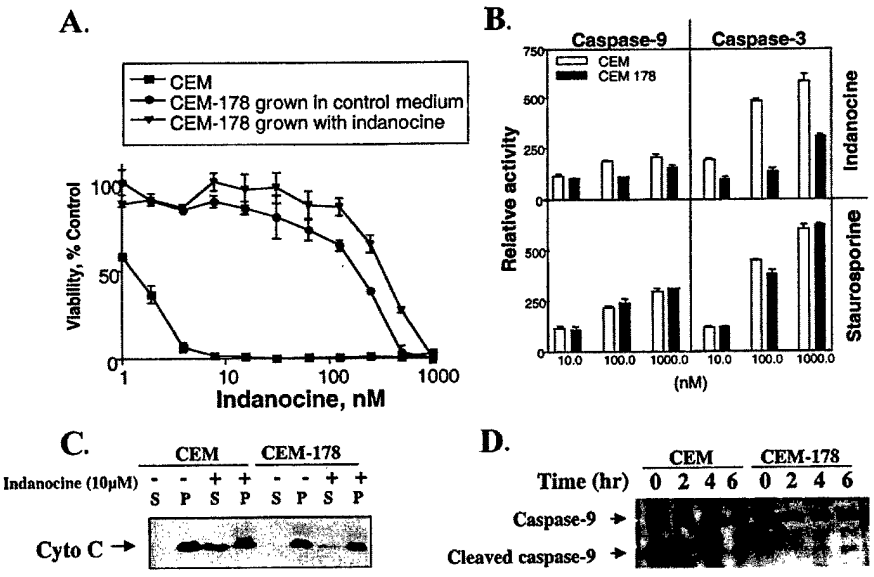

Fig. 1. CEM-178 is resistant to indanocine-induced apoptosis. *A*, CEM wild-type (■), indanocine-resistant CEM-178 out of selection (●) and CEM-178 under selection with indanocine (▼) were treated with increasing concentrations of indanocine for 3 days. Viable cells were assessed by MTT assay. The results are expressed as the percentages of the control values without drug treatment. *Bars*, SD. *B*, CEM wild-type and CEM-178 were assayed for caspase activity after treatment with increasing concentrations of indanocine for 4 h and staurosporine for 16 h. Cells were lysed, and caspase activities were measured by cleavage of specific fluorimetric substrates for caspase-3 and caspase-9. Activities were represented in relative units to the control without treatment. *Bars*, SD. *C*, CEM and CEM-178 cells were each incubated with 10 μM of indanocine for 16 h. The cells were then fractionated into cytosolic and membrane-bound fractions and analyzed by Western blotting. After indanocine treatment, CEM wild-type cells released a significant amount of cytochrome *c* into the cytosol but CEM-178 did not. *Cyto C*, cytochrome C; *S*, sample; *P*, paclitaxel. *D*, CEM and CEM-178 cells were incubated with 10 μM indanocine for the indicated periods of time, lysed, and assayed for caspase-9 cleavage. Whereas indanocine induced caspase-9 cleavage at 4 h, no caspase-9 cleavage was observed for CEM-178.

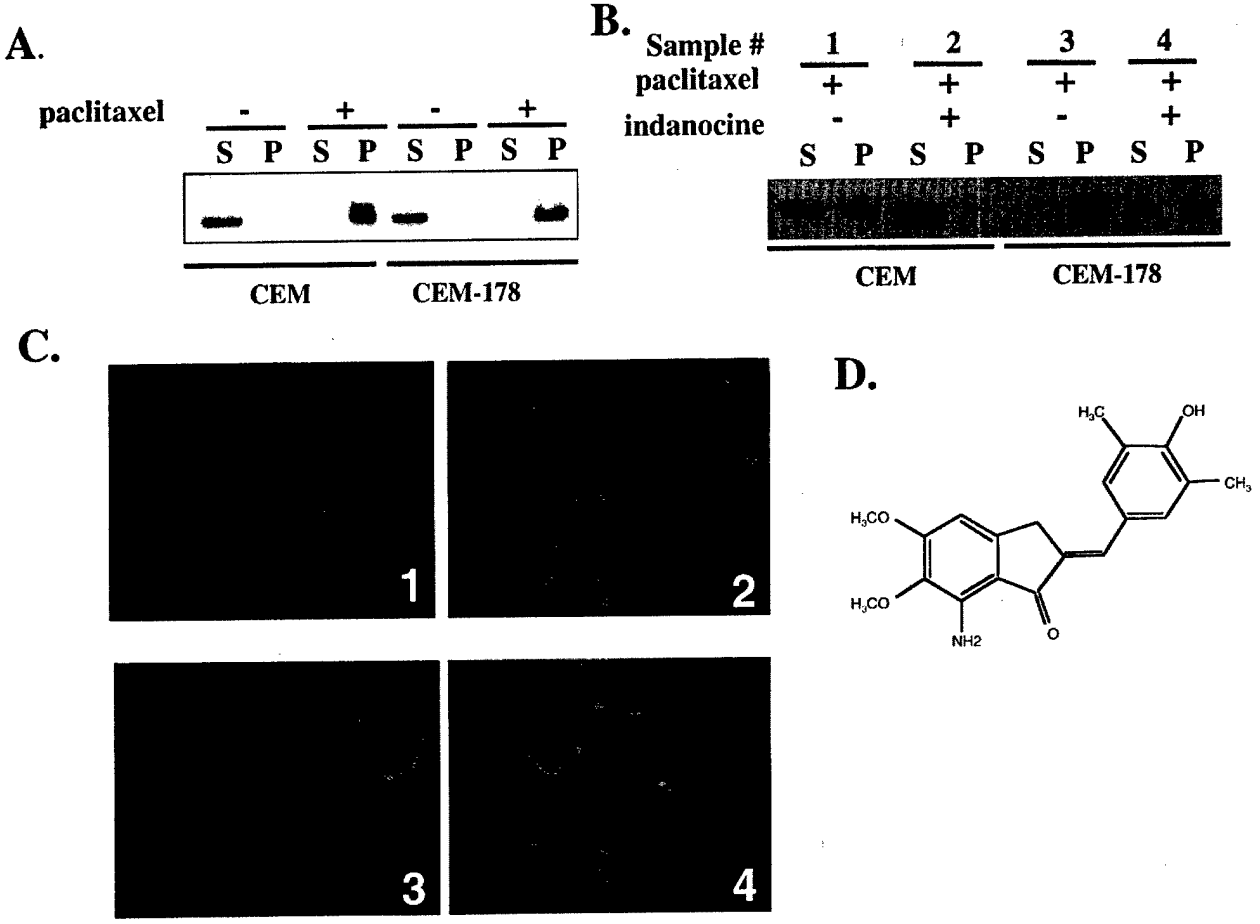

Fig. 2. Indanocine induces tubulin depolymerization in CEM but not CEM-178 cells. *A*, CEM and CEM-178 cells were incubated in medium with or without paclitaxel for 1 h. In both cell types, tubulin existed in a free, cytosolic form. Paclitaxel converted tubulin into polymerized form. *S*, sample; *P*, paclitaxel. *B*, CEM and CEM-178 cells were treated with 5 μM of paclitaxel for 1 h and then washed twice with medium. The cells were then incubated with 10 μM indanocine for 2 h. Soluble and polymerized tubulin were assayed as described in "Materials and Methods." In wild-type CEM cells, polymerized tubulin underwent spontaneous depolymerization, and indanocine treatment completely depolymerized tubulin. In CEM-178 cells, there was no spontaneous depolymerization, and incubation with indanocine depolymerized only a small fraction of tubulin. *S*, sample; *P*, paclitaxel. *C*, CEM and CEM-178 cells were treated as in *B*. The cells were spun onto coverslips and stained for α-tubulin with a monoclonal antibody and with Alexa-568 conjugated secondary antibody (*red*). DNA was visualized with 4′,6-diamidino-2-phenylindole (*blue*). Sample numbers correlate with those of *B*. *D*, structure of indanocine.

merization (Fig. 2*C, panel 2*). The CEM-178 line did not show any visible changes in the microtubule network (Fig. 2*C, panel 4*). Collectively, these results demonstrate that the microtubules in parental CEM and CEM-178 cells react differently to indanocine, and they are consistent with the hypothesis that there is a difference in tubulin structure between CEM and CEM-178 cells.

Cell-free Tubulin Polymerization Assays. To rule out the possibility that CEM-178 resistance might be attributable to a deficiency in drug uptake or active drug metabolism, tubulin depolymerization assays using a cell-free system were performed. Specifically, cells were incubated for 1 h in medium containing 5 μM paclitaxel, washed and lysed in tubulin extraction buffer, and incubated at 37°C for 2 h with 200 μM indanocine, followed by centrifugation and immunoblotting. In parental CEM cells, ~40% of the tubulin was depolymerized by indanocine (Fig. 3*A, CEM*). In contrast, almost all of the tubulin remained in a polymerized form in drug-resistant CEM-178 cells (Fig. 3*A, CEM-178*). It is important to emphasize that the tubulin extracted from CEM-178 cells did not lose its intrinsic ability to depolymerize, because incubation on ice induced a complete depolymerization (data not shown). Because incubating the cell lysate with indanocine made the drug directly accessible to tubulin, this experiment eliminated the possibility that drug uptake or metabolism contributed to indanocine resistance. To determine whether a soluble factor required for tubulin depolymerization was missing or defective in CEM-178 cells, mixing experiments were carried out. After preincubation with paclitaxel, parental CEM and CEM-178 cells were lysed in tubulin extraction buffer containing indanocine. Then, the whole cell lysates from CEM cells were added to a CEM-178 lysate at ratios of 1:1, 1:5, and 1:10. The mixed lysates were incubated at 37°C for 2 h before tubulin depolymerization was assayed. Control experiments confirmed that indanocine induced tubulin depolymerization in the parental CEM lysate (Fig. 3*B, 1:0*) but not in the CEM-178 lysate (Fig. 3*B, 0:1*). When the lysates were mixed, the quantities of soluble tubulin decreased proportionally as the fraction of parental lysate decreased (Fig. 3*B, 1:1, 1:5, 1:10*). Thus, the indanocine-resistant cells did not contain a soluble inhibitor of tubulin polymerization.

Cell Fusion Studies. Cell fusion experiments between CEM-178 and an indanocine-sensitive CEM were carried out to confirm the cytosol mixing experiments. An ouabain-resistant, hypoxanthine phosphoribosyltransferase-negative CEM cell line was hybridized to

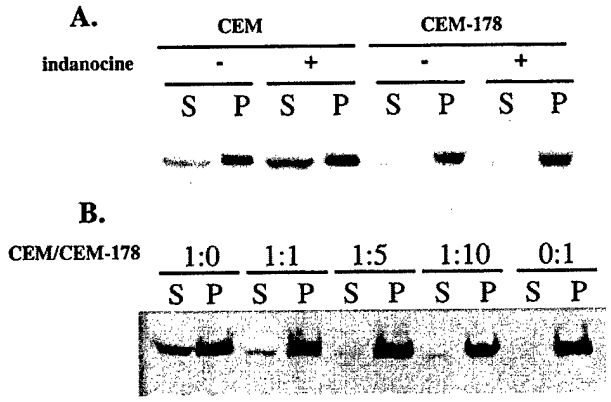

Fig. 3. Mixing experiments. *A*, parental CEM and CEM-178 cells were preincubated with 5 μM paclitaxel for 1 h. The cells were harvested and lysed in a buffer containing 200 μM indanocine and incubated for another 2 h. Then, cytosolic and polymerized tubulin were assayed. Indanocine depolymerized tubulin *in vitro* in CEM cells but not in CEM-178 cells. *S*, sample; *P*, paclitaxel. *B*, CEM and CEM-178 cells were pretreated with paclitaxel and lysed in tubulin extraction buffer with indanocine as in *A*. The lysate from parental CEM cells was mixed with that of CEM-178 at the indicated ratios. The mixed lysates were incubated at 37°C for 2 h and then centrifuged to separate soluble and polymerized tubulin. Tubulin content in each fraction was quantified by Western blotting with a specific anti-α-tubulin antibody. *S*, sample; *P*, paclitaxel.

CEM-178, and heterokaryons were selected and cloned in ouabain-HAT medium. The toxicity of indanocine to several hybridoma clones was between CEM and CEM-178 (Fig. 4*A*). Cross-resistance was partially maintained in the hybridomas (Fig. 4*B*) in that both vinblastine and colchicine were less toxic to the fused cells than to wild-type CEM. These results indicated that the resistance phenotype of the CEM-178 was retained in the fusion cells in a codominant fashion and suggested the possibility of a tubulin mutation.

Sequencing of β-Tubulin b2 and M40 Isotypes. To determine whether a mutation in tubulin was responsible for indanocine resistance, the cDNAs for the two predominant isotypes of β-tubulin, M40 and b2, were sequenced in both directions in both parental CEM and CEM-178 cells. The cDNA sequence of the b2 isotype was identical in the two cell lines and was identical to the GenBank sequence (accession number X02344). In contrast, one point mutation was identified in the cDNA of the M40 isotype, with a G to T substitution at nucleotide 1050 (Fig. 5*B*), which converts amino acid 350 from lysine (AAG) to asparagine (AAU). The mutation was confirmed in two separate amplification and sequencing experiments. The M40 cDNA clone sequence in parental CEM cells was the same as that reported in GenBank (accession number J00314).

DISCUSSION

Indanocine selectively kills malignant B cells at doses that do not affect normal B cells. The CEM-178 mutant lymphoblastoid cell line is resistant to the toxic effects of the tubulin-binding drugs indanocine, vinblastine, and colchicine but is sensitive to paclitaxel. Consistent with this phenotype, CEM-178 cells do not overexpress the multidrug resistance-associated efflux pump Pgp170. Cells that overexpress Pgp170 are indanocine sensitive but paclitaxel resistant (2). Indanocine failed to depolymerize tubulin both in intact CEM-178 cells and in cell-free extracts. Data from extract mixing and cell fusion experiments ruled out the possibility of a missing soluble factor in CEM-178 that is required for indanocine killing but suggested instead that a structural change in tubulin conferred resistance to the drug. In support of this conclusion, a point mutation in β-tubulin, at amino acid 350, was detected in the indanocine-resistant CEM-178 mutant but not in parental cells. The mutation caused a lysine to arginine substitution in the β-tubulin molecule.

The pronounced effect of the point mutation on indanocine toxicity can be explained in at least two ways: (*a*) it is possible that positively charged Lys^{350} represents an important interacting site for indanocine that is lost when changed to Asn; and (*b*) alternatively, it is possible that this mutation changes the overall organization of tubulin, making the microtubule network more rigid. As a result, higher concentrations

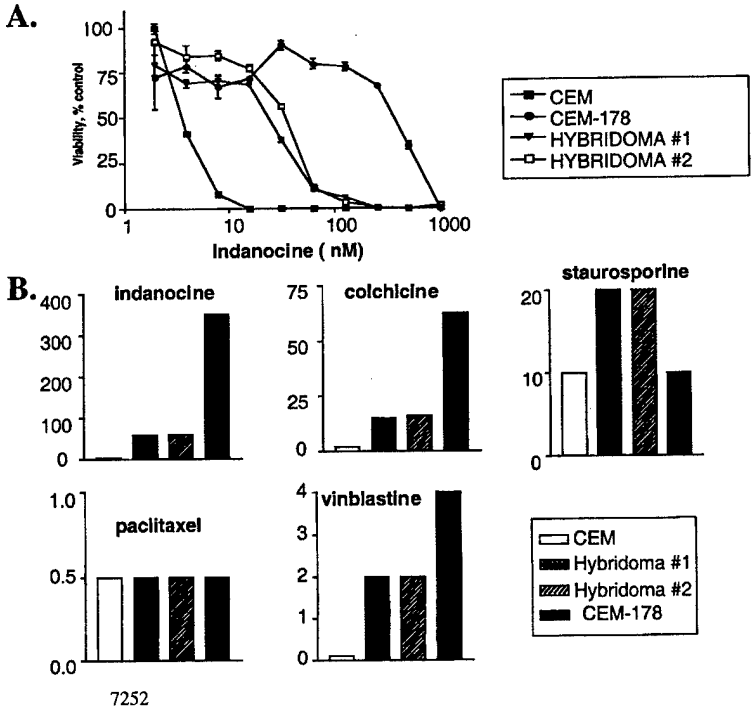

Fig. 4. Indanocine toxicity in hybridoma cell lines and cross-resistance to other drugs. *A*, wild-type CEM (■), indanocine-resistant CEM-178 (●), and two different hybridomas (▼, □) resulting from the fusion of CEM and CEM-178 were assayed for indanocine toxicity. *Bars*, SD. *B*, IC_{50} (in nM) for CEM, CEM-178, hybridoma #1, and hybridoma #2 were plotted for different drugs.

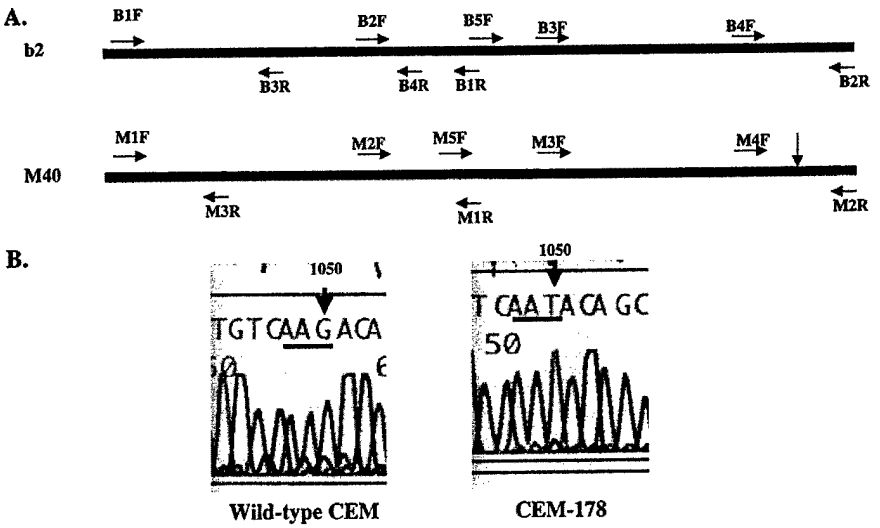

Fig. 5. Sequencing of β-tubulin in CEM-178 reveals a point mutation in the M40 isotype. *A*, schematic diagram of primers used in sequencing of b2 and M40 tubulin. *Vertical arrow*, location of the point mutation. *B*, sequence readout showing that a G residue in position 1050 in wild-type CEM is converted to T in CEM-178.

of indanocine are required to depolymerize the microtubule and to induce cell death. We favor the first mechanism for the following reasons: (*a*) CEM-178 grew normally in regular medium, suggesting that the overall microtubule organization was adequate for rapid cell division; (*b*) Western blot analysis showed that in both CEM and CEM-178 cells, tubulin existed largely in a depolymerized form (Fig. 2*A*). No increased polymerized tubulin was observed in CEM-178; (*c*) if the mutation caused a more rigid microtubule network, it

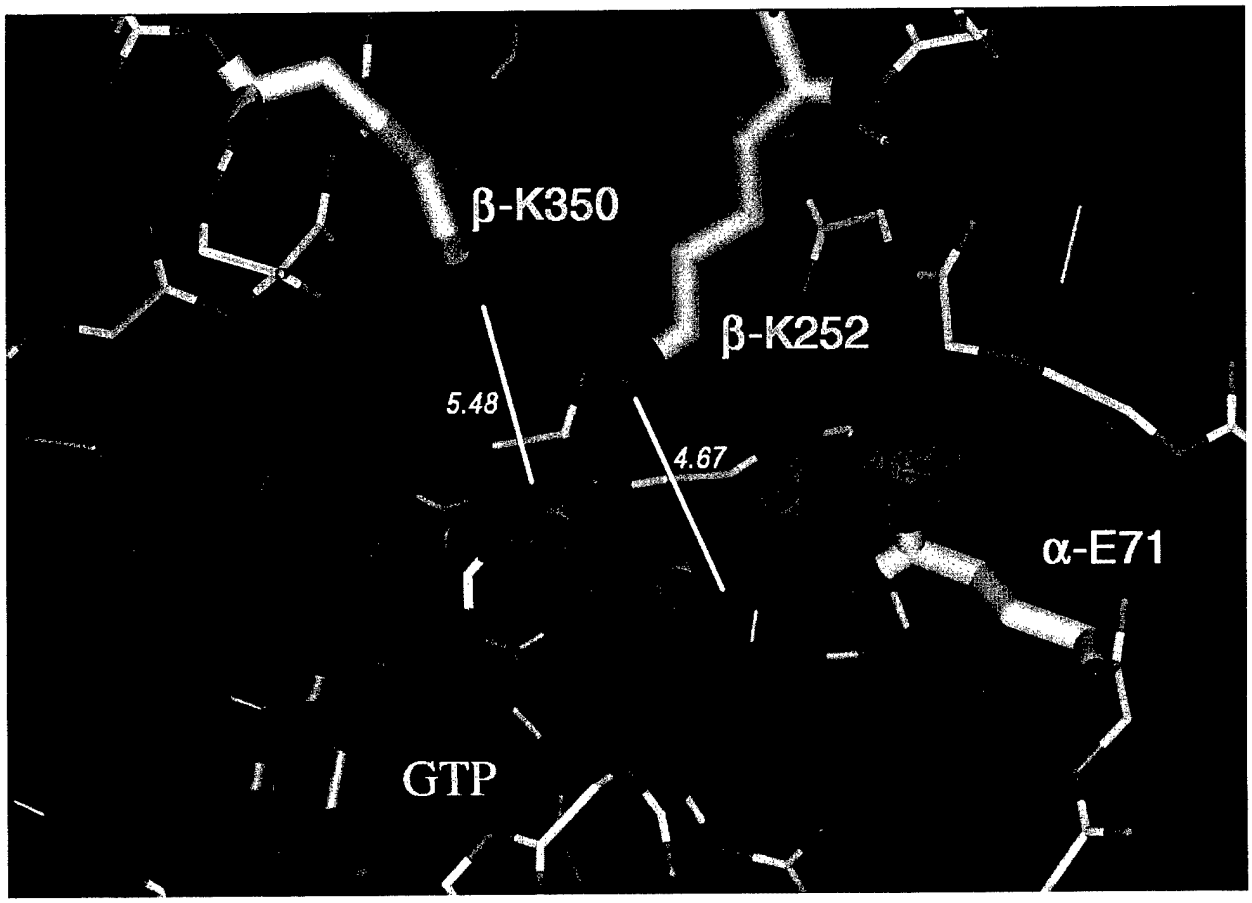

Fig. 6. Proposed electrostatic stabilization of the GTP phosphates by β-K350 of tubulin. The first phosphate is stabilized by the β-K350 (carbons in *cyan*) side chain, the second by β-K252 (carbons in *yellow*) at the shown distances. The terminal phosphate along with the carboxylate of α-E71 (carbons in *yellow*) is stabilized by a Mg^{2+}.

should have increased the threshold for all depolymerizing agents. Therefore, the resistant line should exhibit similar degrees of cross-resistance to other depolymerizing drugs. This is not the case, because CEM-178 is 115-fold more resistant to indanocine but only 40- and 31-fold resistant to vinblastine and colchicine, respectively. Preliminary experiments also have shown that tubulin depolymerization induced by cold temperature occurs at equivalent rates in CEM and the indanocine-resistant mutant (data not shown). Collectively, these results suggest strongly that the identified point mutation on β-tubulin represents a specific interaction site for indanocine.

Increasing evidence from several laboratories suggests that alterations in tubulin primary sequence can play a role in resistance to antimitotic agents. For example, mutations in β270 and β364 have been shown to confer paclitaxel resistance in human ovarian cancer cells (5). Cell lines resistant to epothilone A and B have mutations at β274 and β282 (6).

In contrast to the accumulating knowledge of the paclitaxel-binding site on β-tubulin, the binding sites for colchicine and vinblastine have not been mapped by mutational/molecular modeling approaches. By using light-activated colchicine analogues, Uppuluri *et al.* identified amino acids 214–241 as a probable site for colchicine interaction (11). Other indirect evidence suggests that Cys-354 and Cys-239 play a role in the colchicine binding site (12, 13).

Our results suggest that Lys^{350} might be an important interaction site for indanocine and colchicine. On the basis of the crystal structure of tubulin (14), the α carbon on β-K350 is located only 10 angstroms from the first phosphate group of GTP, which binds near the interface of the α and β monomers. Therefore, we investigated the possibility that β-K350 might provide some functional interaction with GTP, such as charge stabilization. For a fully charged nucleotide or charged amino acid side chain to exist deeply in the interior of a protein, there must be some form of neutralizing bridge. We first observed that the second phosphate group of GTP was already neutralized by the epsilon amino group of β-K252, which is only 4.67 angstroms away. Next, we found that the terminal phosphate of GTP is located very close (4.4 angstroms) to the carboxylate of α-E71 in the Nogales tubulin model (14). On the basis of this observation, as well as the fact that no other basic residues are in the vicinity of α-E71, we formed a model that demonstrates the possibility that a Mg^{2+} can bind and neutralize both α-E71-carboxylate and GTP-terminal phosphate anions. Finally, we were able to modify the dihedral angle of the β-K350, enabling its epsilon amino group to be within 5.48 angstroms from the first phosphate, a distance that favors a stable, neutralizing salt bridge between these two groups. On the basis of the results of these modeling studies, we propose that the β-K350, β-K252 side chains may serve to neutralize the charges of the first two phosphates of GTP at the non-exchangeable site, and that the terminal phosphate along with the carboxylate of α-E71 charges are coneutralized by a Mg^{2+}. Fig. 6 illustrates the results of this model.

Taken together, the results reported in this study explain in part the molecular mechanism of action of indanocine and should facilitate the rational design of other tubulin-binding agents with anticancer activity.

ACKNOWLEDGMENTS

X. H. H. thanks Dr. John Newport (University of California, San Diego, Department of Biology) and Dr. Xu Luo (University of Texas, Southwestern Medical Center, Dallas, TX) for encouragement and many insightful discussions.

REFERENCES

1. Paull, K. D., Lin, C. M., Malspeis, L., and Hamel, E. Identification of novel antimitotic agents acting at the tubulin level by computer-assisted evaluation of differential cytotoxicity data. Cancer Res., *52:* 3892–3900, 1992.
2. Leoni, L. M., Hamel, E., Genini, D., Shih, H., Carrera, C. J., Cottam, H. B., and Carson, D. A. Indanocine, a microtubule-binding indanone and a selective inducer of apoptosis in multidrug-resistant cancer cells. J. Natl. Cancer Inst., *92:* 217–224, 2000.
3. Bosch, I., and Croop, J. P-Glycoprotein multidrug resistance and cancer. Biochim. Biophys. Acta, *1288:* F37–F54, 1996.
4. Pratt, W. B., Ruddon, R. W., Ensminger, W. D., and Maybaum, J. The Anticancer Drugs. New York: Oxford University Press, 1994.
5. Giannakakou, P., Sackett, D. L., Kang, Y. K., Zhan, Z., Buters, J. T., Fojo, T., and Poruchynsky, M. S. Paclitaxel-resistant human ovarian cancer cells have mutant β-tubulins that exhibit impaired paclitaxel-driven polymerization. J. Biol. Chem., *272:* 17118–17125, 1997.
6. Giannakakou, P., Gussio, R., Nogales, E., Downing, K. H., Zaharevitz, D., Bollbuck, B., Poy, G., Sackett, D., Nicolaou, K. C., and Fojo, T. A common pharmacophore for epothilone and taxanes: molecular basis for drug resistance conferred by tubulin mutations in human cancer cells. Proc. Natl. Acad. Sci. USA, *97:* 2904–2909, 2000.
7. Shih, H., Deng, L., Carrera, C. J., Adachi, S., Cottam, H. B., and Carson, D. A. Rational design, synthesis and structure-activity relationships of antitumor (*E*)-2-benzylidene-1-tetralones and (*E*)-2-benzylidene-1-indanones. Bioorg. Med. Chem. Lett., *10:* 487–490, 2000.
8. Liu, X., Kim, C. N., Yang, J., Jemmerson, R., and Wang, X. Induction of apoptotic program in cell-free extracts: requirement for dATP and cytochrome *c*. Cell, *86:* 147–157, 1996.
9. Valentine, M. A., Tsoukas, C. D., Vaughan, J. H., and Carson, D. A. Characterization of Epstein-Barr virus-specific T-cell hybridomas derived from infectious mononucleosis. Clin. Immunol. Immunopathol., *37:* 56–62, 1985.
10. Wetherley-Mein, G., Thomson, A. E., O'Connor, T. W., Peel, W. E., and Singh, A. K. Colchicine ultrasensitivity of lymphocytes in chronic lymphocytic leukaemia. Br. J Haematol., *54:* 111–120, 1983.
11. Uppuluri, S., Knipling, L., Sackett, D. L., Wolff, J. Localization of the colchicine-binding site of tubulin. Proc. Natl. Acad. Sci. *90:* 11598–11602, 1993.
12. Luduena, R. F., and Roach, M. C. Tubulin sulfhydryl groups as probes and targets for antimitotic and antimicrotubule agents. Pharmacol. Ther., *49:* 133–152, 1991.
13. Bai, R., Covell, D. G., Pei, X. F., Ewell, J. B., Nguyen, N. Y., Brossi, A., and Hamel, E. Mapping the binding site of colchicinoids on β-tubulin: 2-chloroacetyl-2-demethylthiocolchicine covalently reacts predominantly with cysteine 239 and secondarily with cysteine 354. J. Biol. Chem., *275:* 40443–40452, 2000.
14. Nogales, E., Wolf, S. G., and Downing, K. H. Structure of the $\alpha\beta$ tubulin dimer by electron crystallography [published erratum appears in Nature (Lond.), *393:* 191, 1998]. Nature (Lond.)., *391:* 199–203, 1998.

ARTICLES

Indanocine, a Microtubule-Binding Indanone and a Selective Inducer of Apoptosis in Multidrug-Resistant Cancer Cells

Lorenzo M. Leoni, Ernest Hamel, Davide Genini, Hsiencheng Shih, Carlos J. Carrera, Howard B. Cottam, Dennis A. Carson

Background: **Certain antimitotic drugs have antitumor activities that apparently result from interactions with nontubulin components involved in cell growth and/or apoptotic cell death. Indanocine is a synthetic indanone that has been identified by the National Cancer Institute's Developmental Therapeutics Program as having antiproliferative activity. In this study, we characterized the activity of this new antimitotic drug toward malignant cells.** ***Methods:*** **We tested antiproliferative activity with an MTT [i.e., 3-(4,5-dimethylthiazol-2-yl)-2,5-diphenyl tetrazolium bromide] assay, mitochondrial damage and cell cycle perturbations with flow cytometry, caspase-3 activation with fluorometry, alterations of the cytoskeletal components with immunofluorescence, and antimicrotubule activity with a tubulin polymerization assay.** ***Results/Conclusions:*** **Indanocine is a cytostatic and cytotoxic indanone that blocks tubulin polymerization but, unlike other antimitotic agents, induces apoptotic cell death in stationary-phase multidrug-resistant cancer cells at concentrations that do not impair the viability of normal nonproliferating cells. Of the seven multidrug-resistant cell lines tested, three (i.e., MCF-7/ADR, MES-SA/DX5, and HL-60/ADR) were more sensitive to growth inhibition by indanocine than were their corresponding parental cells. Confluent multidrug-resistant cells (MCF-7/ADR), but not drug-sensitive cancer cells (MCF-7) or normal peripheral blood lymphocytes, underwent apoptotic cell death 8–24 hours after exposure to indanocine, as measured by sequential changes in mitochondrial membrane potential, caspase activity, and DNA fragmentation. Indanocine interacts with tubulin at the colchicine-binding site, potently inhibits tubulin polymerization *in vitro*, and disrupts the mitotic apparatus in dividing cells.** ***Implications:*** **The sensitivity of stationary multidrug-resistant cancer cells to indanocine suggests that indanocine and related indanones be considered as lead compounds for the development of chemotherapeutic strategies for drug-resistant malignancies. [J Natl Cancer Inst 2000;92:217–24]**

Antimitotic drugs are a major group of antitumor agents, whose varied mechanisms of action have been only partly elucidated *(1)*. Derivatives of natural products, such as the vinca alkaloids, colchicine, cryptophycin, the combretastatins, and related compounds *(2,3)*, as well as several different synthetic heterocyclic compounds *(4,5)*, inhibit tubulin polymerization and prevent microtubule assembly. The taxanes, on the other hand, prevent the depolymerization of tubulin, resulting in the rearrangement of the microtubule cytoskeleton *(6)*. Although some of the antimitotic agents have broad-spectrum cancer chemotherapeutic activity, others, such as colchicine and nocodazole, have no selectivity toward malignant cells. In general, antimitotic agents take advantage of kinetic abnormalities of cancer cells, such as their increased proliferation rate or loss of mitotic checkpoints. Many newer antineoplastic agents focus on biochemical abnormalities that differentiate malignant tumors from most normal tissues *(7–9)*.

The multidrug-resistant phenotype, although not strictly specific for cancer cells, is an attractive target for anticancer drugs because it develops during chemotherapy with bulky hydrophobic antineoplastic agents, limiting their efficacy *(10)*. Several mechanisms may contribute to intrinsic and acquired cross-resistance to multiple antineoplastic agents (clinical drug resistance). They include decreased drug accumulation due to overexpression of the P-glycoprotein drug efflux pump encoded by the mdr1 gene *(11,12)*, the multidrug resistance-associated protein (MRP) *(13)*, and the p110 major vault glycoprotein *(14)*. In addition, multidrug resistance has been linked to decreased expression of topoisomerase IIα *(15)*, to altered expression of drug-metabolizing enzymes and drug-conjugate export pumps *(16,17)*, and to modification of the apoptotic machinery *(18,19)*.

Various hydrophobic drugs with low toxicity for tumor cells can partially reverse multidrug resistance *in vitro* and *in vivo*. In contrast, cytotoxic compounds that preferentially target multidrug-resistant cells are not well described, but such agents should be very useful in the treatment of cancer. The National Cancer Institute's Developmental Therapeutics Program has identified indanocine, a newly synthesized indanone, as a compound with antiproliferative activity.

In this article, we investigate the action of indanocine on cultured multidrug-resistant cancer cells and their corresponding parental (wild-type) cells.

Affiliations of authors: L. M. Leoni, D. Genini, H. Shih, C. J. Carrera, H. B. Cottam, D. A. Carson, Department of Medicine and The Sam and Rose Stein Institute for Research on Aging, University of California San Diego, La Jolla; E. Hamel, Laboratory of Drug Discovery Research and Development, Developmental Therapeutics Program, Division of Cancer Treatment and Diagnosis, National Cancer Institute, National Cancer Institute-Frederick Cancer Research and Development Center, Frederick, MD.

Correspondence to: Lorenzo M. Leoni, Ph.D., Department of Medicine 0663, University of California San Diego, 9500 Gilman Dr., La Jolla, CA 92093 (e-mail: lleoni@ucsd.edu).

See "Notes" following "References."

Materials and Methods

Materials

Indanocine, NSC 698666 (Fig. 1, A), is one of a series of synthetic indanones with antiproliferative activity (Shih H, Deng L, Carrera CJ, Adachi S, Cottam HB, Carson DA: unpublished data). Solid idanocine is a white powder that is stable when stored dry at room temperature or when dissolved in dimethyl sulfoxide or in water containing cyclodextrins. Paclitaxel, vinblastine sulfate, and nocodazole were from Calbiochem (San Diego, CA). Electrophoretically homogeneous bovine brain tubulin was prepared as described previously *(20)*. Media and tissue culture supplies were purchased from Irvine Scientific (Santa Ana, CA) and Fisher Scientific (San Diego, CA). All radiochemicals were from NEN-Dupont (Boston, MA). Unless otherwise indicated, all other reagents were obtained from Sigma Chemical Co. (St. Louis, MO).

Cell Culture

Cell lines from the American Type Culture Collection (Manassas, VA), propagated according to the instructions of the supplier, were as follows: MES-SA (human uterine sarcoma) and its multidrug-resistant variant MES-SA/DX5 raised against doxorubicin *(21)*, monkey COS-1, and Hep-G2 (human hepatocellular carcinoma). KB-3-1 (human carcinoma) and KB-GRC-1 (a transfectoma expressing high levels of the MDR1-encoded 170-kd P-glycoprotein) were provided by Dr. Stephen Howell (University of California San Diego, La Jolla) and have been described previously *(22)*. Dr. Michael J. Kelner (University of California San Diego) provided the following cell lines: MV522 (human metastatic lung carcinoma) and MV522/Q6 (a transfectoma expressing high levels of the MDR1 gene-encoded 170-kd P-glycoprotein); MCF-7/ADR, a human breast adenocarcinoma multidrug-resistant line selected against doxorubicin (expressing both gp170 and the embryonic glutathione transferase π isoform), and MCF-7/wt, the parental (wild-type) line; MDA-MB-231, a human breast adenocarcinoma line, and MDA3-1/gp170+, the doxorubicin-resistant daughter line expressing the 170-kd P-glycoprotein; and HL-60, a human acute promyelocytic leukemia line, and HL-60/ADR, the multidrug-resistant variant line selected against doxorubicin and expressing the MRP/gp180 protein. Dr. William T. Beck (Cancer Center, University of Illinois at Chicago) provided CEM, a human lymphoblastoid line, and CEM/VLB100, a multidrug-resistant line selected against vinblastine and expressing the 170-kd P-glycoprotein.

We incubated cells for 72 hours in 96-well plates with the test compounds and then measured cell proliferation by reduction of the yellow dye MTT [i.e., 3-(4,5-dimethylthiazol-2-yl)-2,5-diphenyl tetrazolium bromide] to a blue formazan product. The cleavage is performed by the "succinate-tetrazolium reductase" system, which belongs to the respiratory chain of the mitochondria and is active only in viable cells. Therefore, the amount of formazan dye formed is a direct indication of the number of metabolically active cells in the culture. The optical density of the blue formazan product was measured at 570 nm with a Thermo-Max (Molecular Devices, Sunnyvale CA) and analyzed with the Vmax Program (BioMetallics, Princeton, NJ).

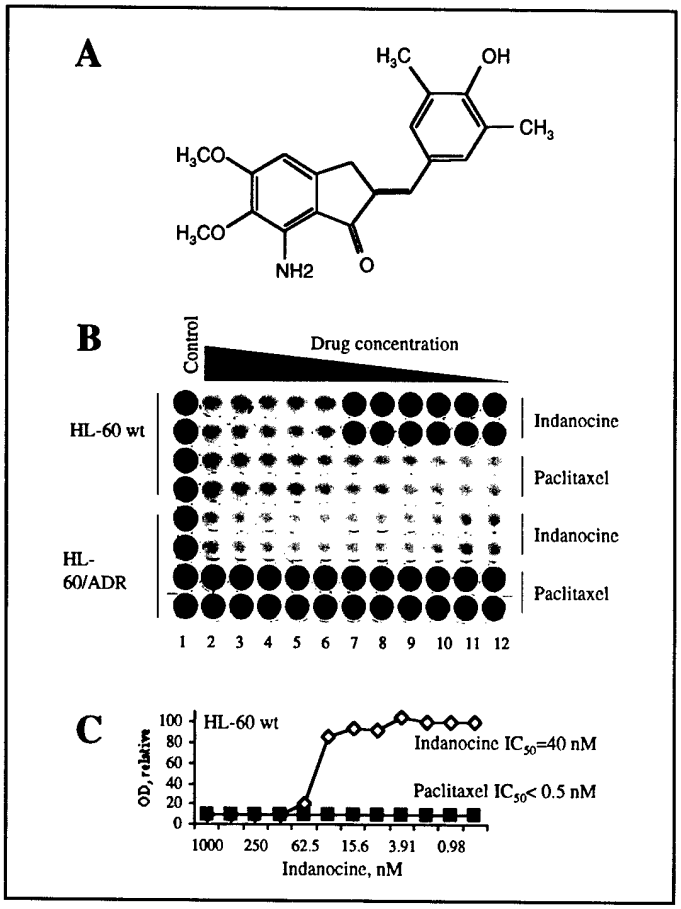

Fig. 1. A) Structure of indanocine. In **panels B** and **C,** HL-60 and HL-60/ADR cells display collateral sensitivity to indanocine; i.e., the multidrug-resistant cell line was substantially more sensitive to the growth-inhibitory effects of indanocine than the original parental cell line. **B)** Cytotoxic MTT [i.e., 3-(4,5-dimethylthiazol-2-yl)-2,5-diphenyl tetrazolium bromide] assay of HL-60 cells. Parental wild-type HL-60 and HL-60/ADR multidrug-resistant cells were plated at low density (<5000 cells per well), and indanocine and paclitaxel were added at 1 : 2 serial dilutions from **column 2. Column 1** is the control without drugs. The initial concentrations were 1 μM for indanocine and 10 μM for paclitaxel, and the concentrations in **column 12** were 1 n*M* and 10 n*M*, respectively. After 3 days, the MTT assay was used to quantitate viable cells. The picture of the plate was obtained by optically scanning the 96-well plate. **Dark wells** represent metabolically active cells, and **clear wells** represent metabolically inactive cells. **C)** Graphic representation of the scanned plate for parental wild-type HL-60 cells, with the calculated 50% inhibitory concentrations (IC_{50}) shown (*see* Table 1).

Cell Cycle Analysis

Cells were harvested, fixed in ice-cold 70% ethanol, treated with ribonuclease A at 100 μg/mL, and stained with propidium iodide at 50 μg/mL for 1 hour at 37 °C. The DNA content of the cells was analyzed by flow cytometry (FACScalibur; Becton Dickinson Immunocytometry Systems, San Jose, CA), and the cell cycle distribution was calculated with the ModFit LT 2.0 Program (Verity Software House, Topsham, ME).

Caspase Analysis

Extracts were prepared by the suspension of 5×10^6 cells in 100 μL of a lysis buffer (i.e., 25 m*M* Tris–HCl [pH 7.5], 150 m*M* KCl, 5 m*M* EDTA, 1% Nonidet P-40, 0.5% sodium deoxycholate, and 0.1% sodium dodecyl sulfate), incubation on ice for 10 minutes, and then centrifugation at 14 000*g* for 5 minutes at 4 °C. The resulting supernatants were collected and frozen at −80 °C or used immediately. Lysates (20 μL containing 5–10 μg of total protein) were mixed with 30 μL of assay buffer [50 m*M* piperazine-*N,N'*-bis(2-ethanesulfonic acid), 50 m*M* KCl, 5 m*M* ethylene glycol bis(β-aminoethyl ether) *N,N,N',N'*-tetraacetic acid, 2 m*M* $MgCl_2$, 1 m*M* dithiothreitol, and 0.1 m*M* phenylmethylsulfonyl fluoride], containing 100 μM of Z-DEVD-AFC (where DEVD is Asp–Glu–Val–Asp, Z is benzyloxycarbonyl, and AFC is 7-amino-4-trifluoromethyl coumarin). Caspase-3-like protease activity was measured at 37 °C with a spectrofluorometric plate reader (LS50B; The Perkin-Elmer Corp., Foster City, CA) in the kinetic mode with excitation and emission wavelengths of 400 nm and 505 nm, respectively. Activity was measured by the release of 7-amino-4-methyl coumarin (AMC) from the synthetic substrate Z-DEVD-AFC (Biomol, Plymouth Meeting, PA).

Mitochondrial Analysis

Cells were treated with the indicated amount of drug and 10 μM Ac-DEVD-fmk (*N*-acetyl-Asp–Glu–ValAsp–fluoromethylketone; Enzyme System Products, Livermore, CA), the cell-permeable caspase-3/caspase-7-selective inhibitor. Cells were then incubated for 10 minutes at 37 °C in culture medium containing 40 n*M* 3,3'-dihexyloxacarbocyanine iodide (DiOC6; Molecular Probes, Inc., Eugene, OR), followed by immediate analysis in a FACScalibur cytofluorometer. Fluorescence at 525 nm was recorded.

Immunofluorescence Assays

Hep-G2 (human hepatocellular carcinoma) cells were grown on glass coverslips in the presence or absence of drugs for 16 hours. Cells were fixed in

paraformaldehyde, permeabilized in Triton X-100, and stained with an anti-β-tubulin monoclonal antibody, followed by tetramethyl rhodamine B isothiocyanate-conjugated anti-mouse immunoglobulin G (IgG). To visualize filamentous actin filaments, we stained the cells with fluorescein isothiocyanate-conjugated phalloidin, as described previously *(23)*. The type 1 nuclear mitotic apparatus protein was detected with monospecific human autoantibodies, as described previously by Andrade et al. *(24)*. The secondary antibody was fluorescein isothiocyanate-labeled goat anti-human IgG (Tago, Burlingame, CA). Nuclei were stained with the DNA-binding dye 4′,6-diamidino-2-phenylindole dihydrochloride (Molecular Probes, Inc.) according to the manufacturer's instructions.

Tubulin Assays

Assessment of the inhibition of tubulin polymerization and the evaluation of the inhibition of [^{3}H]colchicine binding to tubulin were performed as described previously *(25)*. In all experiments, tubulin without microtubule-associated proteins *(20)* was used. In brief, for inhibition of assembly, 10 μ*M* (1.0 mg/mL) tubulin was preincubated with various concentrations of drug (4% [vol/vol] dimethyl sulfoxide as drug solvent) and 0.8 *M* monosodium glutamate for 15 minutes at 30 °C. The reaction mixture was placed on ice, and guanosine 5′-triphosphate (0.4 m*M*) was added. Reaction mixtures were transferred to cuvettes at 0 °C in Gilford 250 spectrophotometers (Beckman-Gilford, Fullerton, CA), baselines were established, and the temperature was increased to 30 °C with electronic temperature controllers (over a period of about 60 seconds). The IC_{50} value is the drug concentration required to inhibit 50% of the assembly, relative to an untreated control sample, after a 20-minute incubation. It should be noted that the bulk of polymer formed in the presence of glutamate consists of sheets of parallel protofilaments. The drug effects in this system are similar to those observed with a preparation containing tubulin and microtubule-associated proteins (i.e., microtubule proteins). The chief advantage of the glutamate system is that it unambiguously establishes tubulin as the drug target. For the colchicine-binding assay, reaction mixtures contained 1.0 μ*M* (0.1 mg/mL) tubulin and 5.0 μ*M* [^{3}H]colchicine and were incubated for 10 minutes at 37 °C before filtration through a stack of two DEAE-cellulose filters. At this time in reaction mixtures without inhibitor, binding is 40%–50% of maximum, so that the inhibition of the rate of colchicine binding to tubulin can be measured accurately.

Results

Inhibition of Cell Growth

In an initial screen performed by the National Cancer Institute's Developmental Therapeutics Program, the mean 50% growth-inhibitory concentration (GI_{50}) of indanocine was less than or equal to 20 n*M*. In 29 of 49 cell lines, including a doxorubicin-resistant breast cancer line, the GI_{50} for indanocine was less than the lowest concentration tested (10 n*M*). Because the indanone is hydrophobic, its activity toward the multidrug-resistant cells was surprising. To confirm this result, we compared the effects of indanocine on the growth of the following pairs of parent and corresponding multidrug-resistant lines (Table 1): MCF-7 and MCF-7/ADR, MES-SA and MES-SA/DX5, MDA-MB-321 and MDA3-1/GP170+3-1, HL-60 and HL-60/ADR, CEM and CEM/VLB100, KB-3-1 and KB-GRC-1, and MV522 and MV522/Q6 cells. The multidrug-resistant cell lines have different multidrug resistance mechanisms, including alterations of gp170 (mdr1 gene), gp180 (MRP gene), and the glutathione transferase π isoform. In several of the cell lines tested, the antiproliferative concentrations of indanocine were equivalent or lower in the multidrug-resistant cells than in the corresponding parent cells. Three of the cell lines tested (i.e., MCF-7, MES-SA, and HL-60) showed collateral sensitivity; i.e., the multidrug-resistant cell line was substantially more sensitive to the growth-inhibitory effects of indanocine than the parental cell line. An example of collateral sensitivity is shown in Fig. 1, where HL-60 and HL-60/ADR cells were plated in a 96-well plate and then treated for 3 days with decreasing (1 : 2 dilutions) concentrations of indanocine (from 1 μ*M*) or paclitaxel (from 10 μ*M*). The MTT assay was then performed at day 3. To prove that P-glycoprotein expression did not confer resistance to the indanone, we compared its effects on two carcinoma cell lines, KB-3-1 and MV522, and their corresponding transfectoma clones that overexpressed P-glycoprotein (the mdr1 gene product), KB-GRC-1 and MV522/Q6 *(22)*. These transfectomas were resistant to paclitaxel, as expected, but retained complete sensitivity to indanocine (Table 1).

Table 1. Growth-inhibitory concentrations of indanocine and paclitaxel in seven multidrug-resistant cell lines*

	GI_{50} (indanocine), n*M*		GI_{50} (paclitaxel), n*M*	
Cell line	Wild type	Mutidrug resistant	Wild type	Multidrug resistant
MCF-7	20 ± 5	4 ± 1†	50 ± 6	>10 000
MES-SA	85 ± 6	12 ± 3†	<1	>1000
MDA-MB-321	10 ± 3	25 ± 2	50 ± 2	>1000
HL-60	40 ± 3	2 ± 0.2†	<1	>1000
CEM	12 ± 2	20 ± 1	<1	606 ± 20
KB-3-1	7 ± 2	7 ± 3	7 ± 3	>1000
MV522	13 ± 3	8 ± 2	15 ± 4	358 ± 58

*The cells were treated with various concentrations of indanocine or paclitaxel for 72 hours. Cell proliferation was assessed by the MTT [i.e., 3-(4,5-dimethylthiazol-2-yl)-2,5-diphenyl tetrazolium bromide] assay. The results represent the 50% growth-inhibitory concentrations (GI_{50}) (mean ± standard deviation; n > 5). The human breast adenocarcinoma MCF-7/ADR cell line was selected against doxorobucin and expresses both gp170 and the embryonic glutathione transferase π isoform. The human uterine sarcoma line MES-SA/DX5 line was selected against doxorobucin *(21)*. The doxorubicin-resistant human breast adenocarcinoma cell line MDA3-1/gp170+ expresses the 170-kd P-glycoprotein. The human acute promyelocytic leukemia line HL-60/ADR was selected against doxorobucin and expresses the MRP/gp180 protein. The human lymphoblastoid CEM/VLB100 line was selected against vinblastine and expresses the 170-kd P-glycoprotein. The transfectoma KB-GRC-1 expresses high levels of the MDR1-encoded 170-kd P-glycoprotein *(22)*. The metastatic human lung transfectoma MV522/Q6 expresses high levels of the MDR1-encoded 170-kd P-glycoprotein.

†$P<.001$ versus wild-type value by Wilcoxon signed rank test.

Effect of Indanocine on Stationary-Phase Cells

The results obtained with the actively growing parent and multidrug-resistant cell lines led us to test indanocine in stationary-phase cell lines. As determined by flow cytometry after propidium iodide staining, up to 81% of stationary MCF-7/ADR cells (1 week in confluent culture) were in the G_1 phase of the cell cycle (Fig. 2, B; middle panel). Remarkably, indanocine treatment of stationary-phase multidrug-resistant cells, but not parental cells, resulted in cell death (IC_{50} = 32 n*M*) (Fig. 2, A). The cytotoxic effect of indanocine in noncycling MCF-7/ADR cells was confirmed by the detection of an apoptotic sub-G_0/G_1 population by flow cytometry and by the activation of caspase-3 (Fig. 2, B; left panel). Parental (wild-type) MCF-7 cells were similarly growth arrested but did not show apoptotic features (data not shown). In addition, normal peripheral blood lymphocytes exposed to 1000-fold higher concentrations of indanocine for 72 hours showed no loss of viability (data not shown).

Apoptosis

The study described above demonstrated that stationary MCF-7/ADR cells, but not wild-type MCF-7 cells, were sensitive to treatment with indanocine. To test this observation in

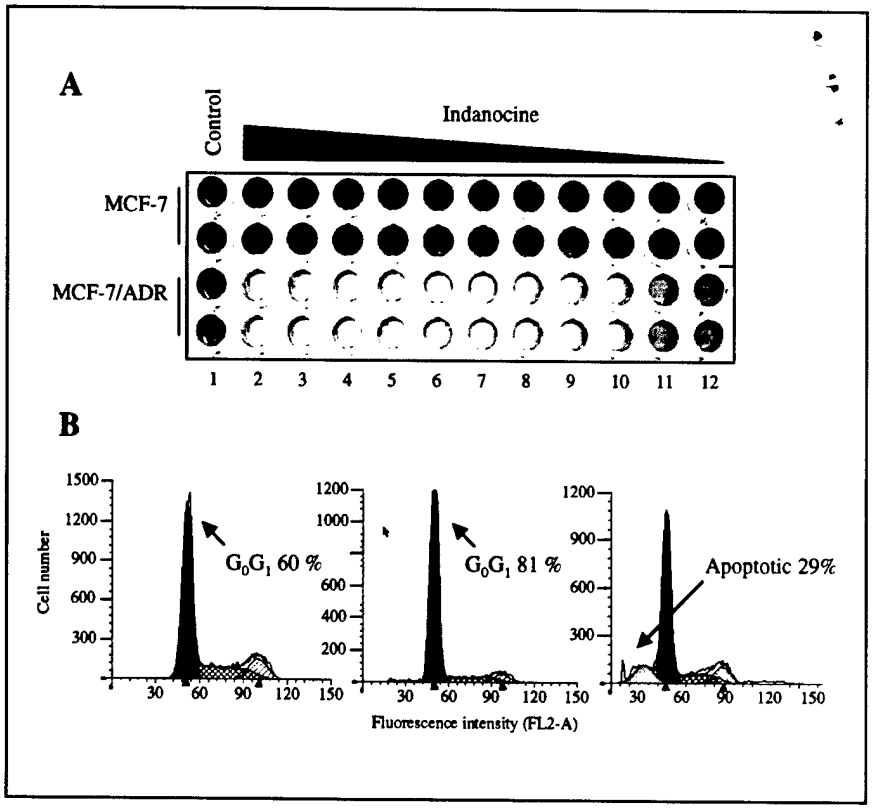

Fig. 2. Effect of indanocine on resting multidrug-resistant cells. **A**) Toxicity of indanocine on resting MCF-7 cells. Parental wild-type MCF-7 and MCF-7/ADR multidrug-resistant cells were maintained in a confluent state for 7 days by daily replacement of the medium. Indanocine was then added at 10 μM in wells in **column 2** and serially diluted 1 : 2 in each successive column (reaching 10 nM in **column 12**). **Column 1** is the control, without indanocine. After 3 days, the MTT [i.e., 3-(4,5-dimethylthiazol-2-yl)-2,5-diphenyl tetrazolium bromide] assay was used to quantitate viable cells. **B**) DNA content and caspase activity of indanocine-treated cells. MCF-7/ADR multidrug-resistant cells were harvested, permeabilized, and stained with propidium iodide. The DNA content of cells was established by flow cytometry. **Solid peak** = cells in the G_0/G_1 phase; **cross-hatched peak** = cells in the S phase; **hatched peak** = cells in the G_2/M phase; **shaded peak** (present only in the **right panel**) = hypodiploid, apoptotic cells, as modeled with the ModFit Program. At the **left** are normally proliferating cells, in the **middle** are confluent cells (7 days), and at the **right** are indanocine-treated, growth-arrested confluent MCF-7/ADR cells. The percentage of cells that are in G_0/G_1 phase or that are apoptotic is indicated. The relative caspase activity is the fluorometric measurement of the caspase-3-like activity normalized to the control cells (**left**). For normally proliferating MCF-7/ADR cells, the relative caspase activity is 100; for 7-day confluent MCF-7/ADR cells, it is 100; for growth-arrested, confluent MCF-7/ADR cells treated with indanocine, it is 450.

another cell line pair that displayed collateral sensitivity to indanocine in the multidrug-resistant derivative line, we selected HL-60 and HL-60/ADR cells because of the exquisite sensitivity of HL-60/ADR cells to indanocine. In the experiment shown in Fig. 3, we tested the ability of indanocine to activate caspase-3 in parental and multidrug-resistant HL-60 cells. Caspase-3, considered an "executioner" caspase, is implicated in the last and irreversible phase of the apoptotic caspase pathway and is activated by upstream "initiator" caspases, such as caspase-8 and caspase-9 [reviewed in *(26)*]. Caspase activity was measured by use of the fluorogenic caspase-3-specific substrate DEVD-AMC. HL-60/ADR cells incubated with 10 nM indanocine showed a time-dependent increase in caspase-3 activity compared with untreated cells, reaching a maximum at 24 hours. In contrast, wild-type HL-60 cells showed only a slight increase in caspase-3 activity, about 25% of that obtained in the multidrug-resistant cells (Fig. 3, A).

To determine the effect of indanocine treatment on the mitochondrial transmembrane potential of multidrug-resistant and wild-type cells, we used the fluorochrome DiOC6 (Fig. 3, B). In apoptosis induced by various stimuli, a decrease in the mitochondrial transmembrane potential has been shown to precede nuclear DNA fragmentation *(27)*. The flow cytometry results showed a visible reduction in DiOC6 fluorescence for HL-60/ADR cells incubated with indanocine for 8 hours, indicating that the mitochondrial transmembrane potential in these cells was reduced. After 16 hours, the percentage of cells with reduced DiOC6 fluorescence had reached 44%. HL-60 wild-type cells incubated with the same amount of indanocine did not display the same strong reduction in DiOC6 fluorescence.

Effect on Tubulin Polymerization

Indanocine did not change the flow cytometry profile of stationary-phase cells stained for DNA, other than to cause the appearance of hypodiploid apoptotic cells in multidrug-resistant cultures (Fig. 2). However, concentrations of the drug that inhibited cell proliferation caused a rapid increase in the number of cells in G_2/M phases in growing cultures (data not presented).

Antimitotic drugs usually interfere with cellular microtubules by interacting with tubulin *(3)*. Using glutamate-induced assembly of purified tubulin (containing no microtubule-associated proteins) as our assay, we found (Fig. 4, A) that indanocine inhibited tubulin assembly in a manner comparable to that of nocodazole rather than inducing polymerization as would paclitaxel. This observation led us to perform a quantitative analysis (Fig. 4, B), in which we found that indanocine was nearly as potent as combretastatin A-4 (a gift of Dr. G. R. Pettit, Arizona State University, Tempe, AZ) as an inhibitor of tubulin assembly. We measured the extent of tubulin assembly after a 20-minute incubation at 30 °C and determined that the IC_{50} of combretastatin A-4 was 1.20 ± 0.03 μM (mean ± standard deviation; n = 4) and that the IC_{50} of indanocine was 1.7 ± 0.1 μM (n = 3). Both compounds practically eliminated the binding of 5 μM [^{3}H]colchicine to 1 μM tubulin when present at 5 μM—combretastatin A-4 inhibited 98% ± 4% of colchicine binding (n = 4), and indanocine inhibited 95% ± 2% of colchicine binding (n = 4). The effects of various concentrations of the two drugs on colchicine binding are shown in Fig. 4, C. Neither agent inhibited the binding of [^{3}H]vinblastine to tubulin (single experiment).

Cytoskeletal Effects of Indanocine

COS-1 and Hep-G2 cells were grown on glass coverslips and treated with various concentrations of indanocine, nocodazole, or vinblastine sulfate. The microtubule network was then visualized by indirect immunofluorescence with an anti-β-tubulin antibody, and the microfilament network was stained with fluorescein isothiocyanate-coupled phalloidin. COS-1 and Hep-G2

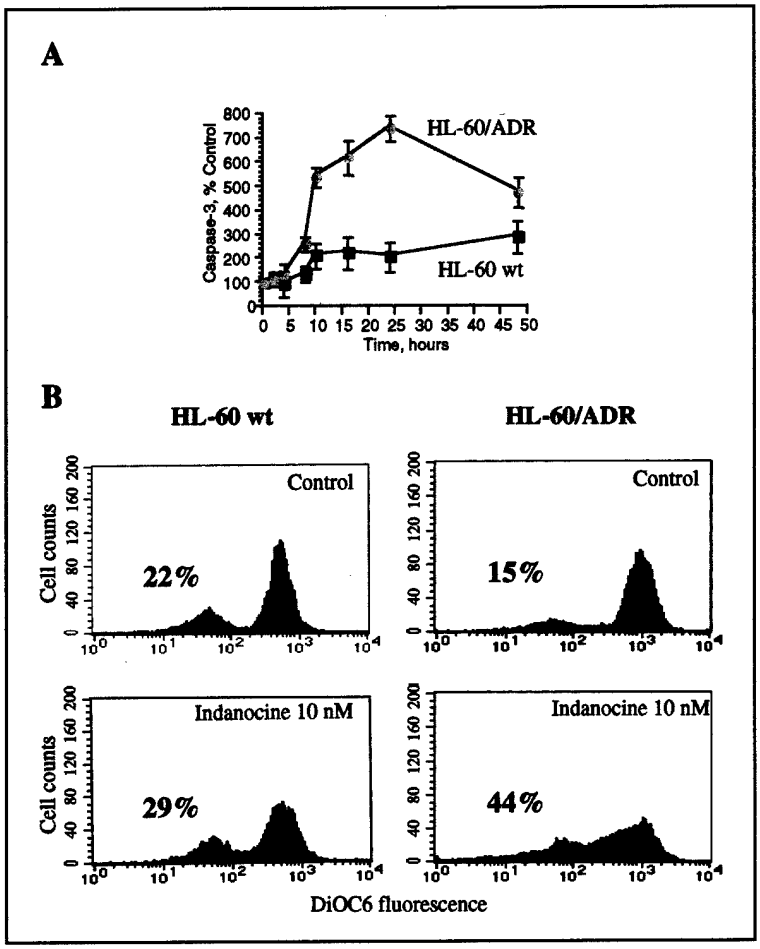

Fig. 3. Indanocine induces apoptosis in multidrug-resistant cells. **A)** Activation of caspase-3 by indanocine. HL-60 wild-type (wt) and multidrug-resistant (ADR) cells were treated with 10 n*M* indanocine; at the indicated times, caspase-3-like activity was measured with the specific fluorogenic substrate DEVD-AMC (Asp–Glu–Val–Asp coupled to 7-amino-4-methyl coumarin). The results are expressed as the means ± standard deviation (**error bars**) and are representative of up to four experiments. **B)** Reduction of mitochondrial transmembrane potential by indanocine. HL-60 cells were treated with and without indanocine at 10 n*M*. After 16 hours of incubation, cells were incubated with 40 n*M* 3,3′-dihexyloxacarbocyanine iodide (DiOC6), followed immediately by flow cytometry in a FACScalibur. The ***x*-axis** represents the DiOC6 fluorescence. The ***y*-axis** represents the number of cells. The percentage of low-DiOC6 fluorescence-gated cells is indicated.

cells were used for these studies because of their clearly defined microtubule and microfilament networks, respectively. Untreated cells had extensive microtubule systems with perinuclear organizing centers (Fig. 5, a and b) and had microfilament bundles and stress fibers that were predominantly aligned with the major axis of the cell (Fig. 6, a and b).

Treatment of COS-1 cells with 0.5 or 5 μ*M* indanocine for 1 hour depleted the cells of microtubules, resulting in diffuse cytoplasmic staining with anti-β-tubulin antibody (Fig. 5, c and d). Treatment with 0.55 μ*M* (0.5 μg/mL) vinblastine sulfate (Fig. 5, f) for 1 hour had a similar effect. Modifications induced by 3.3 μ*M* (1 μg/mL) nocodazole (Fig. 5, e) for 1 hour were less pronounced, and some of the perinuclear organizing centers were still visible.

Indanocine-treated Hep-G2 cells had a rounded shape, and the microfilament cytoskeleton in these cells was disorganized, characteristic of treatment with a depolymerizing agent (Fig. 6, c). After a 1-hour incubation in 0.5 μ*M* indanocine, some cells

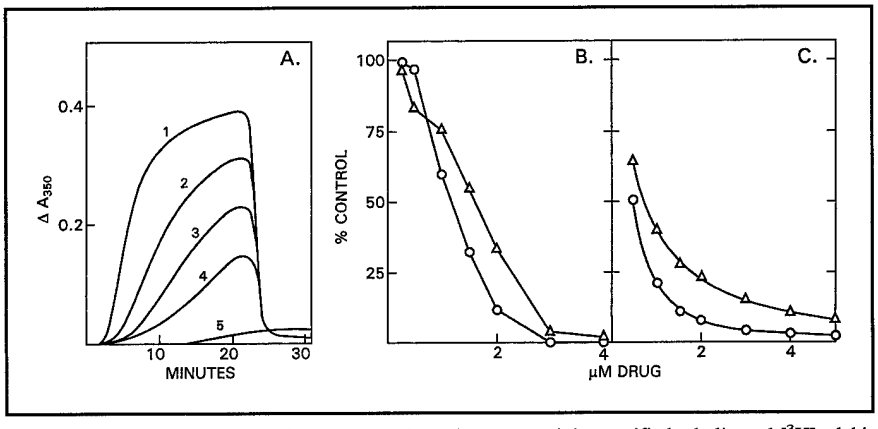

Fig. 4. Effect of indanocine on tubulin polymerization and binding of [^{3}H]colchicine to tubulin. Absorbance was measured at 350 nm (A_{350}). Inhibition of tubulin polymerization (**A** and **B**) and inhibition of [^{3}H]colchicine binding to tubulin (**C**) by indanocine and by combretastatin A-4. **Panel A:** For the tubulin polymerization assay, tubulin (10 μ*M*) was incubated with indanocine at the following concentrations: 0 for **curve 1,** 1.0 μ*M* for **curve 2,** 1.5 μ*M* for **curve 3,** 2.0 μ*M* for **curve 4,** and 3.0 μ*M* for **curve 5.** At 0 time, the temperature controller was set at 30 °C for 20 minutes to measure polymerization; at 20 minutes, the temperature controller was set at 0 °C to measure the amount of cold-reversible tubulin polymer formation. **Panels B** and **C:** Concentrations of indanocine (△) and combretastatin A-4 (○) were as indicated. **Panel B:** Values obtained for the inhibition of tubulin polymerization in all experiments were averaged. For 1.0, 1.5, and 2.0 μ*M* drug, there were four values for combretastatin A-4 and five for indanocine. There were fewer experimental values for the other concentrations. The mean control A_{350} value in these experiments was 0.382. **Panel C:** Indanocine inhibition of [^{3}H]colchicine binding to tubulin. In this assay, indanocine was added at various concentrations to a reaction mixture containing purified tubulin and [^{3}H]colchicine and incubated for 10 minutes at 37 °C. The amount of [^{3}H]colchicine bound to tubulin was then measured after filtration on DEAE-cellulose. The experiment shown in panel C was performed once with duplicate samples for each data point.

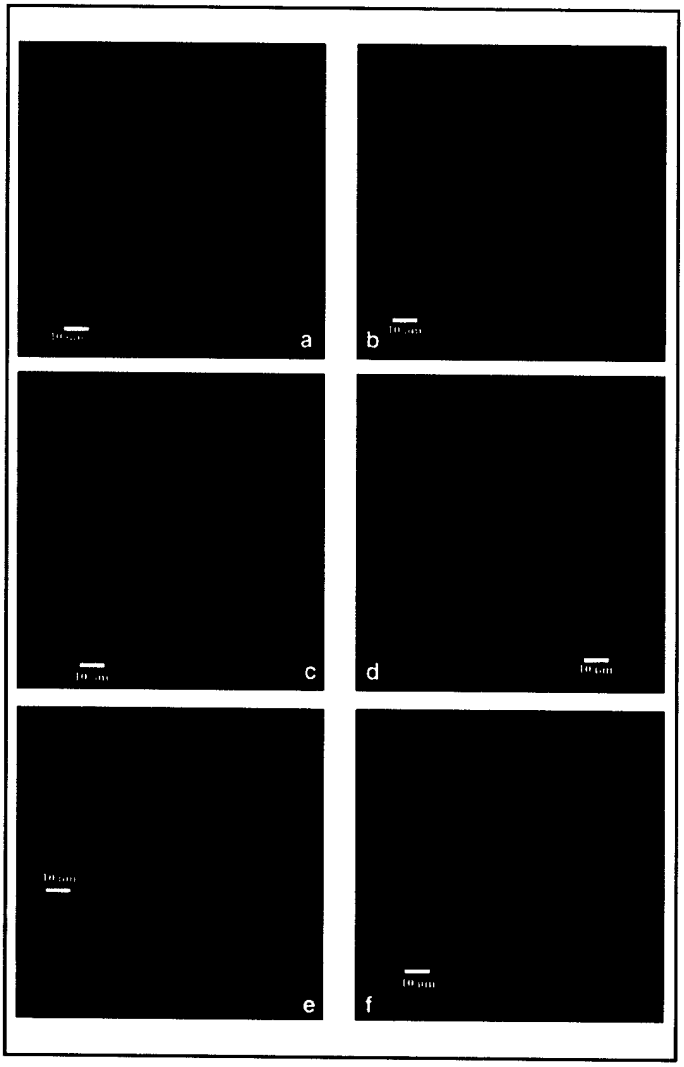

Fig. 5. Effect of indanocine on the microtubular network. COS-1 cells were incubated for 2 hours with dimethyl sulfoxide (**a**) or ethanol (**b**), 5 μM and 500 nM indanocine (**c** and **d**, respectively), 3.3 μM (1 μg/mL) nocodazole (**e**), or 0.55 μM (0.5 μg/mL) vinblastine sulfate (**f**). The cells were fixed, microtubules were labeled (**red**) with an anti-β-tubulin antibody, and nuclei were stained (**blue**) with 4′,6-diamidino-2-phenylindole dihydrochloride.

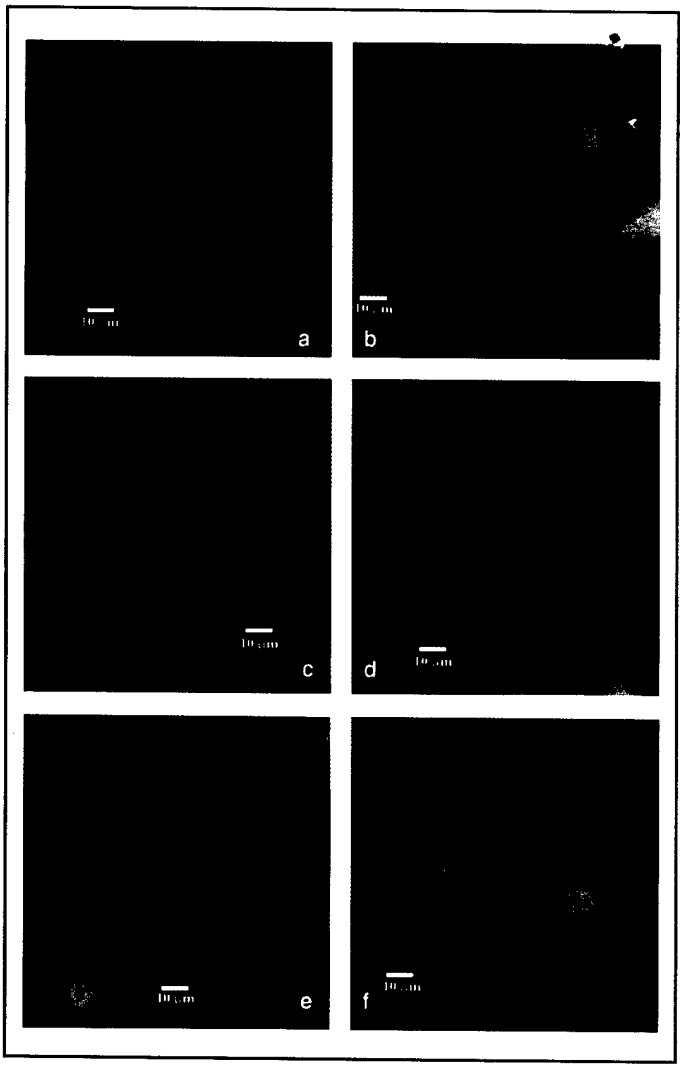

Fig. 6. Effect of indanocine on the microfilament network. Hep-G2 cells were incubated for 2 hours with dimethyl sulfoxide (**a**) or ethanol (**b**), 5 μM and 500 nM indanocine (**c** and **d**, respectively), 3.3 μM (1 μg/mL) nocodazole (**e**), and 0.55 μM (0.5 μg/mL) vinblastine sulfate (**f**). Cells were fixed, microfilaments were stained with fluorescein isothiocyanate-coupled phalloidin (**green**), and nuclei were stained with 4′,6-diamidino-2-phenylindole dihydrochloride (**blue**).

had a characteristic rounded shape, but other cells had normal microfilament bundles (Fig. 6, d). A similar effect was observed after exposure to nocodazole (Fig. 6, e) or vinblastine sulfate (Fig. 6, f). This is probably an indication that the microfilament breakdown observed at 5 μM indanocine is not a direct effect but rather is a consequence of the rapid and potent disruption of the microtubule network.

After treatment of Hep-G2 cells with 100 nM indanocine, the subcellular localization of the mitotic apparatus (as shown by human autoantibodies against the type 1 nuclear mitotic apparatus protein) was determined by immunofluorescence. In control cells undergoing mitosis, the type 1 nuclear mitotic apparatus protein was localized at the poles of the mitotic spindle (Fig. 7, a). In cells exposed to 100 nM indanocine and arrested in the M phase, type 1 nuclear mitotic apparatus protein was distributed in spots scattered over the nucleus (Fig. 7, b). A similar effect was observed with 3.3 μM nocodazole (Fig. 7, c). Paclitaxel treatment did not interfere with the subcellular distribution of the type 1 nuclear mitotic apparatus protein, although it affected the formation of a functional mitotic spindle (Fig. 7, d).

Discussion

Indanocine is a derivative of indanone with antiproliferative activity (Shih H, Deng L, Carrera CJ, Adachi S, Cottam HB, Carson DA: unpublished data). An initial screen of malignant cell lines performed by the National Cancer Institute's Developmental Therapeutics Program and the COMPARE Program *(28)* suggested that these compounds had tubulin-binding properties. In this screening, the indanones, including indanocine, retained activity toward multidrug-resistant breast cancer cells. Indanocine interacts with tubulin at the colchicine-binding site, and it inhibits tubulin polymerization with an IC_{50} value equivalent to values obtained with podophyllotoxin and combretastatin A-4 *(29)*. Consistent with these biochemical effects, in intact cells, indanocine disrupts intracellular microtubules including those of the mitotic spindle and leads to redistribution of the components of the nuclear mitotic apparatus. The discrepancy between the micromolar concentration of drug required for *in vitro* inhibition of tubulin polymerization and the nanomolar concentrations of drug that blocked cell proliferation has been

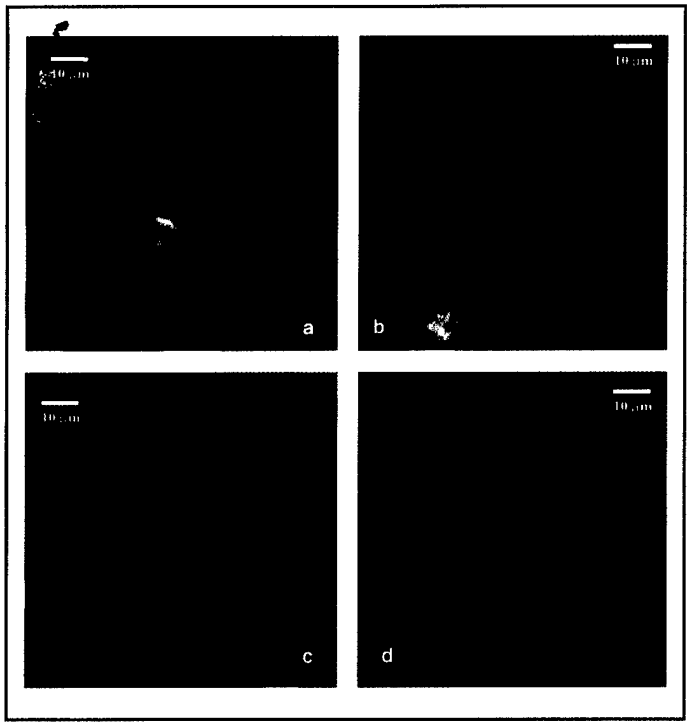

Fig. 7. Effect of indanocine on type 1 nuclear mitotic apparatus protein. Hep-G2 cells were incubated for 16 hours with dimethyl sulfoxide (**a**), 0.1 μ*M* indanocine (**b**), 3.3 μ*M* (1 μg/mL) nocodazole (**c**), or 0.1 μ*M* paclitaxel (**d**). Cells were fixed and labeled with monospecific human autoantibodies to type 1 nuclear mitotic apparatus protein.

observed with other antitubulin agents *(5,25,29)*. This discrepancy may indicate that indanocine interacts with other nontubulin cellular components to produce a cytotoxic response. This hypothesis is supported by the ability of short-term treatment with indanocine to trigger apoptosis in stationary multidrug-resistant cancer cells (whose survival should not depend on DNA synthesis or an intact mitotic apparatus) but not in control cells.

Modification of the apoptotic machinery has been proposed as an explanation for the *de novo* and acquired cross-resistance to multiple antineoplastic agents. It has been shown that the Bcl-2 protein may protect cancer cells from drug-induced apoptotic cell death *(18,30,31)*. Microtubule-disrupting drugs, such as vincristine, vinblastine, and colchicine, and microtubule-stabilizing drugs, such as paclitaxel and doxetaxel, induce growth arrest, which is followed by phosphorylation and inactivation of Bcl-2, which eventually leads to apoptotic cell death in the G_2/M phase of the cell cycle *(32–34)*. In contrast, cells in the stationary phase are generally resistant to many of these agents, and phosphorylation of Bcl-2 in the G_0/G_1 phase is generally not observed. This property limits the utility of tubulin-binding drugs for the treatment of malignant tumors containing only a few proliferating cells (i.e., tumors with a low S-phase fraction).

As with other microtubule-damaging drugs, indanocine arrested the growth of multidrug-sensitive cancer cells at the G_2/M boundary and induced apoptotic cell death. The nanomolar concentrations of indanocine that induced apoptosis in multidrug-resistant cells did not kill wild-type G_1-phase cancer cells or quiescent normal peripheral blood lymphocytes. Nanomolar concentrations of indanocine forced stationary, multidrug-resistant cells into the apoptotic program. That these cells were arrested in the G_0/G_1 phase of the cell cycle was confirmed by cytofluorometric analysis. Apoptosis, in these cells, was confirmed by the appearance of a subdiploid-DNA flow-cytometry peak and by caspase-3 activation. Compared with their respective parental lines, five multidrug-resistant cell lines displayed higher or indistinguishable sensitivity to indanocine toxicity.

The cell lines hypersensitive to indanocine have modified various systems for multidrug resistance. MES-SA/DX5 cells overexpress P-glycoprotein, and MCF-7/ADR cells overexpress P-glycoprotein and also have an embryonic π isoform of glutathione transferase *(35)*. HL-60/ADR cells express the MRP/gp180 protein. The other two cell lines that we examined, with unaltered sensitivity to indanocine, only express P-glycoprotein.

The fact that sensitivity to indanocine was retained by all of the multidrug-resistant cells tested, including both KB-3-1 and MV522 transfectomas that overexpress the P-glycoprotein, suggests that this agent acts independently of the P-glycoprotein hydrophobic multidrug transporter and/or that the cytoskeletal disorganization induced by the indanone interfered with P-glycoprotein functions. In other experiments, indanocine did not alter the rate of rhodamine efflux from loaded cells (data not shown). Thus, it seems probable that the uptake and regulation of indanocine do not depend on or directly influence the P-glycoprotein multidrug transporter.

Several different microtubule-disrupting agents have been developed that do not depend on the 170-kd P-glycoprotein and that display antiproliferative activity against multidrug-resistant cancer cells *(23,36)*. It should be of interest to determine whether any of these agents, like indanocine, are cytotoxic to noncycling mdr1-expressing cells. Such comparative studies could answer the question whether the mechanism of action of indanocine is related only to inhibition of microtubule function. If indanocine-induced cell death involves another intracellular target, then other microtubule-disrupting agents with antiproliferative activity toward multidrug-resistant cells should not be able to induce apoptosis in the G_0/G_1 phase.

The observation that indanocine kills noncycling, multidrug-resistant cells has practical implications. The low percentage of cycling cells in many human solid tumors limits the potential of antimitotic drugs. The combination of a drug that is selectively cytotoxic to nondividing, multidrug-resistant cells and an antineoplastic agent that kills tumors with abnormalities of cell cycle checkpoints could represent an exceptionally effective approach to eradicating malignant cells while sparing most normal tissues. Thus, we suggest that indanocine and related indanones be considered lead compounds for the development of chemotherapeutic strategies for drug-resistant malignancies.

References

(1) Rowinsky EK, Donehower RC. The clinical pharmacology and use of antimicrotubule agents in cancer chemotherapeutics. Pharmacol Therap 1991;52:35–84.

(2) Sinha S, Jain S. Natural products as anticancer agents. Prog Drug Res 1994;42:53–132.

(3) Hamel E. Antimitotic natural products and their interactions with tubulin. Med Res Rev 1996;16:207–31.

(4) Cushman M, He HM, Lin CM, Hamel E. Synthesis and evaluation of a series of benzylaniline hydrochlorides as potential cytotoxic and antimitotic agents acting by inhibition of tubulin polymerization. J Med Chem 1993; 36:2817–21.

(5) Xia Y, Yang ZY, Xia P, Bastow KF, Tachibana Y, Kuo SC, et al. Anti-

tumor agents. 181. Synthesis and biological evaluation of 6,7,2′,3′,4′-substituted-1,2,3,4-tetrahydro-2-phenyl-4-quinolones as a new class of antimitotic antitumor agents. J Med Chem 1998;41:1155–62.
(6) Adams JD, Flora KP, Goldspiel BR, Wilson JW, Arbuck SG, Finley R. Taxol: a history of pharmaceutical development and current pharmaceutical concerns. J Natl Cancer Inst Monogr 1993;21:141–7.
(7) Jordan VC. Tamoxifen treatment for breast cancer: concept to gold standard. Oncology (Huntingt) 1997;11:7–13.
(8) Mangues R, Corral T, Kohl NE, Symmans WF, Lu S, Malumbres M, et al. Antitumor effect of a farnesyl protein transferase inhibitor in mammary and lymphoid tumors overexpressing N-ras in transgenic mice. Cancer Res 1998;58:1253–9.
(9) Arguello F, Alexander M, Sterry JA, Tudor G, Smith EM, Kalavar NT, et al. Flavopiridol induces apoptosis of normal lymphoid cells, causes immunosuppression, and has potent antitumor activity *in vivo* against human leukemia and lymphoma xenografts. Blood 1998;91:2482–90.
(10) Ling V. Multidrug resistance: molecular mechanisms and clinical relevance. Cancer Chemother Pharmacol 1997;40 Suppl:S3–8.
(11) Bosch I, Croop J. P-glycoprotein multidrug resistance and cancer. Biochim Biophys Acta 1996;1288:F37–54.
(12) Higgins CF. The multidrug resistance P-glycoprotein. Curr Opin Cell Biol 1993;5:684–7.
(13) Loe DW, Deeley RG, Cole SP. Biology of the multidrug resistance-associated protein, MRP. Eur J Cancer 1996;32A:945–57.
(14) Izquierdo MA, Scheffer GL, Flens MJ, Schroeijers AB, van der Valk P, Scheper RJ. Major vault protein LRP-related multidrug resistance. Eur J Cancer 1996;32A:979–84.
(15) Wessel I, Jensen PB, Falck J, Mirski SE, Cole SP, Sehested M. Loss of amino acids 1490Lys–Ser–Lys1492 in the COOH-terminal region of topoisomerase IIalpha in human small cell lung cancer cells selected for resistance to etoposide results in an extranuclear enzyme localization. Cancer Res 1997;57:4451–4.
(16) Kawasaki H, Carrera CJ, Piro LD, Saven A, Kipps TJ, Carson DA. Relationship of deoxycytidine kinase and cytoplasmic 5′-nucleotidase to the chemotherapeutic efficacy of 2-chlorodeoxyadenosine. Blood 1993;81:597–601.
(17) Goker E, Waltham M, Kheradpour A, Trippett T, Mazumdar M, Elisseyeff Y, et al. Amplification of the dihydrofolate reductase gene is a mechanism of acquired resistance to methotrexate in patients with acute lymphoblastic leukemia and is correlated with p53 gene mutations. Blood 1995;86:677–84.
(18) Strasser A, Huang DC, Vaux DL. The role of the bcl-2/ced-9 gene family in cancer and general implications of defects in cell death control for tumourigenesis and resistance to chemotherapy. Biochim Biophys Acta 1997;1333:F151–78.
(19) Hickman JA. Apoptosis and chemotherapy resistance. Eur J Cancer 1996;32A:921–6.
(20) Hamel E, Lin CM. Separation of active tubulin and microtubule-associated proteins by ultracentrifugation and isolation of a component causing the formation of microtubule bundles. Biochemistry 1984;23:4173–84.
(21) Chen G, Duran GE, Steger KA, Lacayo NJ, Jaffrezou JP, Dumontet C, et al. Multidrug-resistant human sarcoma cells with a mutant P-glycoprotein, altered phenotype, and resistance to cyclosporins. J Biol Chem 1997;272:5974–82.
(22) Shalinsky DR, Andreeff M, Howell SB. Modulation of drug sensitivity by dipyridamole in multidrug resistant tumor cells *in vitro*. Cancer Res 1990;50:7537–43.
(23) Smith CD, Zhang X, Mooberry SL, Patterson GM, Moore RE. Cryptophycin: a new antimicrotubule agent active against drug-resistant cells. Cancer Res 1994;54:3779–84.
(24) Andrade LE, Chan EK, Peebles CL, Tan EM. Two major autoantigen-antibody systems of the mitotic spindle apparatus. Arthritis Rheum 1996;39:1643–53.
(25) Verdier-Pinard P, Lai JY, Yoo HD, Yu J, Marquez B, Nagle DG, et al. Structure–activity analysis of the interaction of curacin A, the potent colchicine site antimitotic agent, with tubulin and effects of analogs on the growth of MCF-7 breast cancer cells. Mol Pharmacol 1998;53:62–76.
(26) Salvesen GS, Dixit VM. Caspases: intracellular signaling by proteolysis. Cell 1997;91:443–6.
(27) Castedo M, Hirsch T, Susin SA, Zamzami N, Marchetti P, Macho A, et al. Sequential acquisition of mitochondrial and plasma membrane alterations during early lymphocyte apoptosis. J Immunol 1996;157:512–21.
(28) Paull KD, Lin CM, Malspeis L, Hamel E. Identification of novel antimitotic agents acting at the tubulin level by computer-assisted evaluation of differential cytotoxicity data. Cancer Res 1992;52:3892–900.
(29) Chen K, Kuo SC, Hsieh MC, Mauger A, Lin CM, Hamel E, et al. Antitumor agents. 178. Synthesis and biological evaluation of substituted 2-aryl-1,8-naphthyridin-4(1H)-ones as antitumor agents that inhibit tubulin polymerization. J Med Chem 1997;40:3049–56.
(30) Ringborg U, Platz A. Chemotherapy resistance mechanisms. Acta Oncol 1996;35 Suppl 5:76–80.
(31) Reed JC, Miyashita T, Takayama S, Wang HG, Sato T, Krajewski S, et al. BCL-2 family proteins: regulators of cell death involved in the pathogenesis of cancer and resistance to therapy. J Cell Biochem 1996;60:23–32.
(32) Haldar S, Chintapalli J, Croce CM. Taxol induces bcl-2 phosphorylation and death of prostate cancer cells. Cancer Res 1996;56:1253–5.
(33) Srivastava RK, Srivastava AR, Korsmeyer SJ, Nesterova M, Cho-Chung YS, Longo DL. Involvement of microtubules in the regulation of Bcl2 phosphorylation and apoptosis through cyclic AMP-dependent protein kinase. Mol Cell Biol 1998;18:3509–17.
(34) Blagosklonny MV, Giannakakou P, el-Deiry WS, Kingston DG, Higgs PI, Neckers L, et al. Raf-1/bcl-2 phosphorylation: a step from microtubule damage to cell death. Cancer Res 1997;57:130–5.
(35) Moscow JA, Townsend AJ, Goldsmith ME, Whang-Peng J, Vickers PJ, Poisson R, et al. Isolation of the human anionic glutathione *S*-transferase cDNA and the relation of its gene expression to estrogen-receptor content in primary breast cancer. Proc Natl Acad Sci U S A 1988;85:6518–22.
(36) Bollag DM, McQueney PA, Zhu J, Hensens O, Koupal L, Liesch J, et al. Epothilones, a new class of microtubule-stabilizing agents with a taxol-like mechanism of action. Cancer Res 1995;55:2325–33.

NOTES

Supported in part by a grant from the Swiss National Science Foundation; by Public Health Service grants GM23200 (National Institute of General Medical Sciences) and CA78040-01 (National Cancer Institute), National Institutes of Health, Department of Health and Human Services; and by a grant from the Novartis corporation.

Manuscript received June 29, 1999; revised November 4, 1999; accepted November 18, 1999.